journal of the international meteor organization

WGN

47:6
december 2019

International Meteor Conference 2019 report
Shower activity profiles inferred from radiant density ratios
Possible recurring feature in the Geminid stream
Two southern meteor showers discovered by BRAMON
October IMO video meteors

ISSN 1016-3115

WGN Vol. 47, No. 6, December 2019, pp. 165 – 192

Conferences

Meteor science

Preliminary results

Front cover photo

Fireball over water on 2019 July 24 from Piermont, New Hampshire USA. This object was widely seen over the northeastern USA and Canada. Photo courtesy: Ross Phelps.
For more information on this fireball visit: `https://fireball.imo.net/members/imo_view/event/2019/3151`.

Writing for WGN

This Journal welcomes papers submitted for publication. All papers are reviewed for scientific content, and edited for English and style. Instructions for authors can be found in WGN **45:1**, 1–5, and at `http://www.imo.net/docs/writingforwgn.pdf` .

Legal address

International Meteor Organization, Jozef Mattheessensstraat 60, 2540 Hove, Belgium.

Conferences

International Meteor Conference 2019 report

Mohammed Fadil Talafha [1]

Received 2019 December 5

Introduction

This was my first visit to Germany. I had heard a lot about this beautiful country and I very much wanted to visit it. This was the IMC's first attractive point for me.

A year ago, my colleagues and I built the meteor observation stations in the United Arab Emirates, funded by UAESA and operated by SAASST. We start collecting data in September 2018 and during that time we were dependent on reading papers and brainstorming in order to develop our expertise. I started to look for any institute or organization that could help me establish whether I was doing things the right way and also to gain more information that would help develop our work in meteor observing. Indeed, after a year of observation, with more than 12000 data files, we had created a simple procedure to calculate orbits for the meteors that we had recorded and to establish which of these belonged to meteor showers.

In order to be more accurate in our work and to develop our experience in this field, we need to meet people who have experience in this type of work. Unfortunately, in our region there is no history of work in this field of research. Consequently, I started looking on the internet to find any good source that would guiding me in meteor observing and I found the International Meteor Organization (IMO). I started looking through their website and I found the advertisement for the next conference (IMC 2019) in Germany. I immediately decided to attend this conference in order to meet people with expertise in meteor observation and analysis, and that is what happened.

In fact, it is a part of our job description in the University of Sharjah and it is also university policy that we must discuss our planned conference visits with our supervisor. In our first meeting, I made clear my interest in attending the IMC and he immediately agreed because he knows that we need to establish international links and to meet the professionals. After that, everything moved smoothly, including the submission of my visa application, the booking of my airplane ticket, my conference registration and also many meetings with my colleagues to identify the points that we needed to learn more about from this conference.

An important point regarding my attending of this conference was that I am the first Arab researcher to have participated in this field since 2004.

The trip from UAE (Dubai) to Germany (Bollmannsruh)

I started my trip with an early flight on Thursday 3rd of October at 9:00 AM from Dubai international airport with a direct flight to Hamburg International airport. It took 6 hours and 30 minutes. I arrived on the same day at 13:45 PM. I then traveled by train from Hamburg to Berlin, and from Berlin it took one-hour to Bollmannsruh, the town that was holding the conference. I arrived at 8:30 PM.

The organizers were very helpful, when I met them. They helped me receive my room key and they did everything to enable a comfortable stay.

First day at the conference

After breakfast on the Friday morning, the first presentation started at 9:00 AM. I was waiting to give my presentation, which was scheduled for 14:45, and would describe our work in the field of meteor observing.

From the outset, I began to recognize and understand the experience of the presenters and their work in the field of meteor observation. Many of these presentations highlighted my need to increase my experience as many of the presenters had a long history in meteor observation and analysis.

Figure 1 – The author presenting his team.

[1] Email: mtalafha@sharjah.ac.ae

IMO bibcode WGN-476-talafha-imc2019 NASA-ADS bibcode 2019JIMO...47..165T

I noted my points from each presenter, and I asked them during the floor time for question or after that in the coffee breaks. They were very helpful and kind people and answered all of my questions.

When it came to the time for my presentation, I presented our work in front of all attendees and I felt that they were interested and surprised by our efforts. They asked me many questions in order to find out more about our meteor observing stations and how we manage this work with a big working team. I feel very proud of what we did. All attendees wished the best for me and my team for our hard work.

My lecture

Although this was the first time that I'd presented our work internationally, the friendly atmosphere in the presentation class made me feel confident. My presentation, which started at 14:45, explained everything we work on, but although there were many experts in attendance, they still wanted to know more about the project. I answered four questions and left the rest of the questions to discuss in a coffee break. That discussion actually lasted all three days of the conference.

Figure 2 – The author during his lecture.

Things I Liked

Really, I was very grateful to be in Germany, and the gentle hospitality made me feel like a member of the family. I was also really impressed by the final report of the Conference. It was very clear and professional. The trip to Potsdam it was amazing. We visited the first observation site for Einstein, large telescopes (solar & visual). I liked the weather with rain because I missed it. The place where we stayed during the IMC was very quiet in the early morning and that motivated me to take walks. The charming nature of the venue made me want to attend many more conferences.

Interaction with other participants

I met most of the participants either scientifically or informally during the lunch breaks. I came to the scientific parts with many questions seeking answers. In fact, I not only found the answers but learned much more. I appreciated that.

My first discussion was about a fireball above Germany. I asked about the analysis of the observations and the determination of the trajectory. A second topic involved the discussion of new camera systems and how we need to upgrade our system in UAE. The third important discussion concerned how we in the UAEMMN project can increase our number of double detections via the many suggestions people were making to me. These included reprogramming to fine the dark flight projection by Python, collaboration with a specialist from Russia to test new cameras for our system and starting collaboration with FRIPON network by holding cameras in our towers.

Figure 3 – Participants of IMC 2019.

I gained much new knowledge during the conference, including 3-D meteor trails and many ideas about how to look for and collect meteorites from the desert. All of this matches my desire for scientific work regarding meteors and meteorites and gives me a push to work harder and more professionally.

Back to UAE and After

On the last day at the conference, I felt that I still needed more time to get more advice from the experts. I am still in touch with many of them to discuss many points. I really made new friendships during this short time and I believe they will last a long time. I, or one of my colleagues, hope to be at the upcoming IMC in 2020 to share our latest results and to meet our meteor family.

From the Treasurer — IMO Membership/WGN Subscription Renewal for 2020

Marc Gyssens

Renewal rates

Most members/subscribers whose membership/subscription has expired should have received a reminder email. Via this way, we invite them again to renew for 2020.

The fees are as tabulated below. We are happy that we can offer WGN at the same cost as last year. We also continue to offer an electronic-only subscription at a reduced rate.

IMO Membership/WGN Subscription 2020				
Electronic + paper with surface mail delivery:		€26		US$ 32
Electronic + paper with airmail delivery (outside Europe only):		€49		US$ 60
Electronic only:		€21		US$ 25
Supporting membership:	add	€26	add	US$ 32

It is also possible to renew for two or more years in a row.

When you renew, give a few minutes of thought to becoming a **supporting member** by paying at least 26 EUR/32 USD extra. Smaller gifts are of course also appreciated. As you may know, there is an IMO Support Fund. With this Support Fund, we offer support to meteor-related projects. Our ability to provide this service to the meteor community depends primarily on the gifts we receive from supporting members!

Another way to help meteor workers with limited funds is to offer them a gift subscription.

We already thank all our members that will renew for their continued trust in our Organization!

Payment instructions

If you are not yet familiar with the new IMO website, you first must log in into your account if you want to renew. For this purpose, click the log-in button in the upper right-hand corner. As login, use the email address on which you received my reminder email. In case you forgot your password, you can use the "forgot password" link to reset it. Once logged in, you will see your profile picture (or the space provided for it). If you read on the green button below it that your membership is about to expire, click it, and the rest will be self-explanatory.[1]

The outcome of this process is that you will see the total amount due and your payment options. If you choose to pay using PayPal (or using a credit card via PayPal), you can complete the payment on our website.

If you experience any difficulties, do not hesitate to contact me at `treasurer@imo.net`.

One final request: every year, a lot of members renew late. As a consequence, back issues that already appeared have to be sent out to these members. Please support our volunteers in their bimonthly effort to have WGN shipped to you by renewing promptly! Thank you for your understanding and cooperation!

[1] Alternatively, you can also click on "Extend your membership" in the pull-down menu to the right of your name in the upper right-hand corner, with the same result.

Meteor science

Profiles of meteor shower activities inferred from the radiant Density Ratios (DR)

Masahiro Koseki [1]

The density ratio (DR) of radiants makes it possible to understand activity profiles of meteor showers. The DR is expressed by the radiant density ratio of the number of radiants within 3° to the number of radiants between 3° and 6° usually. The former density implies the intensity of the shower activity and the latter the background intensity. It is not necessary to take the radiant shift into consideration in many cases when we use the sun centered ecliptic coordinates ($\lambda - \lambda_s$, β). We confirmed that the DR is a strong tool for meteor activity studies by surveying Capricornids and Geminids for example. The DR is a useful tool especially to confirm the existence of very weak meteor activity and to define the detectable period of its activity against the background. We can reveal the activity profiles of many famous but minor meteor showers in terms of visual observations by using the DR derived from video observations of SonotaCo net (SonotaCo, 2009): κ-Cygnids, Ursids, σ-Hydrids, η-Hydrids, Andromedids, December Monocerotids, November Orionids, Leonis Minorids, ε-Geminids, January Comae Berenicids, July Pegasids, September ε-Perseids, ζ-Cassiopeids.

Received 2019 October 23

1 Introduction

We are used to express meteor shower activities as ZHR curves (profiles) from visual observations but there are few profiles drawn from video observations. ZHR curves are calculated in case of major meteor showers when an observer can record several meteors an hour. It is natural that video observers can draw similar profiles in such cases, though they usually intend to calculate orbital elements and not to give profiles. Video observations revealed many minor meteor showers but they could detected a few member meteors during all night long. We can get mean radiants, velocity and orbital data of such minor showers; IAUMDC Meteor Shower Database (SD, 2018; this study used the Jan 13 20:35:17 2018 version) lists the mean position of the radiant and the mean solar longitude of the observed meteors; it is not the time of the activity maximum.

The author indicated that the DR is useful for studying meteor activities (Koseki, 2018, 2019a). We can avoid observational deviations by using the DR; the bias of observations affected by weather or sky conditions can be compensated by comparing the radiant density around the mean radiant point with the surrounding radiant density. This paper shows the profiles of several meteor showers and the efficiency of DR especially for minor shower studies.

2 Procedures

The Capricornids (CAP) are not a major shower in visual observations but video observations have caught many CAP meteors. The activity profile of CAP has been uncertain because of the low hourly rates of CAP in visual observations. CAP is a suitable example for explaining the procedures of DR calculation and its usefulness; video observations and the DR method can show clear activity profile of CAP. We applied the following procedures for each of the selected meteor showers; the radiant distributions and the profiles are drawn on the basic data given in Table 1. The common procedures are omitted in each section in order to explain the results briefly: the interval and the center of the radiant distribution, the meaning of the density ratio of the radiants, the calculation of the radiant shift and so on.

2.1 Selection of the proper radiant position and the solar longitude of the activity

It is necessary to select the tentative data from the SD at first. The SD has several entries for each meteor shower but they are uncertain in several cases. We use the median value of them as the tentative center and not

Table 1 – Median values of the meteor showers selected from the SD in this study.

Name and Code	λ_s [°]	$\lambda - \lambda_s$ [°]	β [°]
Capricornids (CAP)	125.55	179.4	9.7
Geminids (GEM)	261.5	208.0	10.4
κ-Cygnids (KCG)	141	161.2	74.5
Ursids (URS)	270.6	218.5	72.1
σ-Hydrids (HYD)	259.1	230.9	−16.8
η-Hydrids (EHY)	257.6	237.5	−14.7
Andromedids (AND)	229.5	163.1	19.8
Dec. Monocerotids (MON)	261	202.2	−14.8
November Orionids (NOO)	246.05	203.8	−8.1
Leonis Minorids (LMI)	209	297.9	26.0
ε-Geminids (EGE)	205.05	255.0	4.4
Jan. Comae Berenicids (JCO)	302.5	240.9	18.8
July Pegasids (JPE)	109.95	244.2	14.4
September ε-Perseids(SPE)	168	248.8	20.4
ζ-Cassiopeids (ZCS)	112.3	277.8	43.0

[1]The Nippon Meteor Society 4-3-5 Annaka-shi, AnnakaGunma-ken, 379-0116 Japan.
Email: geh04301@nifty.ne.jp

IMO bibcode WGN-476-koseki-profiles
NASA-ADS bibcode 2019JIMO...47..168K

the peculiar entries (Table 1). Therefore it is necessary to convert the radiant data (α, δ) into ($\lambda - \lambda_s$, β) using the median solar longitude of the activity.

2.2 Calculation of the distance from the selected point (center): radiant distribution and the profile

Usually, the radiant point is represented in right ascension and declination (α, δ) and its shift with the solar longitude as well. Figure 1a shows the radiant distribution of CAP in (α, δ). The radiants are distributed in an ellipse and this figure suggests the radiant shifts with time.

We calculate the distance from the selected point expressed in ($\lambda - \lambda_s$, β) and draw the radiant distribution between 10 degrees before and after the selected (central) solar longitude of the activity. Figure 1b shows the same CAP data in the sun centered ecliptic coordinates ($\lambda - \lambda_s$, β) and the distribution ellipse becomes smaller. It is clear that we should represent the radiant point in ($\lambda - \lambda_s$, β) and not in (α, δ): the y-axis runs through the median $\lambda - \lambda_s$ (scales are in degrees). We count the number of radiant points according to the distance from the center in ($\lambda - \lambda_s$, β). We draw also the estimated profile by the number of meteors radiants within 3° from the center (Nr $\leq$ 3; in short N3 hereafter) and the DR. DR is the radiant density ratio of the central 3° to the ring between 3° and 6° (DR3; in short DR hereafter). The sliding mean of the 3° bin of λ_s is used here because of the scarcity of radiants in the outer range. Figure 2a shows the activity profiles represented by N3, DR and the number of originally classified CAP meteors by SonotaCo. When the radiant distribution and the profile are not good for the selected data, it is necessary to select suitable entry in the SD near to the center in the radiant positions and in the activity period.

2.3 Calculation of the linear regression of $\lambda - \lambda_s$ and β on λ_s

The radiant distribution in Figure 1b appears still elongated as in many other cases. This ellipse occurs due to the radiant shift in the period of $\Delta\lambda_s = 20$, though the elliptic shape of a radiant distribution is natural in some cases. We test whether the radiant drift is real by calculating the preliminary linear regression of $\lambda - \lambda_s$ and β on λ_s. We select the radiant data in 6° distance from the center, because the radiants are dispersed by the drift itself and the radiant point is tentative. We calculate the linear regression in the period° before and after the selected median λ_s. If we would calculate it for a longer time span, the results might be dispersed by the uncertainty of the tentative data.

2.4 Calculation of the radiant distribution around the estimated center

In this step we use the estimated radiant point calculated by the linear regression as the center and we can obtain a revised radiant distribution and the revised profile. Figure 1c (radiant distribution) and 2b

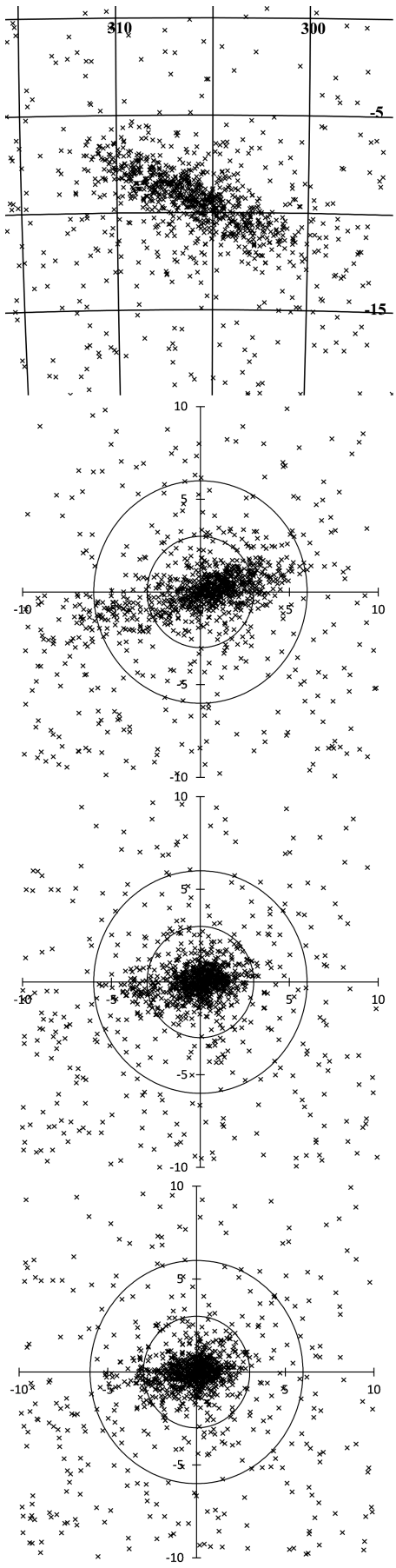

Figure 1 – The radiant distribution of CAP. (a) in (α, δ), (b) in ($\lambda - \lambda_s$, β) without a correction for the radiant shift (the radius of two circles are 3° and 6°), (c) in ($\lambda - \lambda_s$, β) estimated from the first linear regression and (d) in ($\lambda - \lambda_s$, β) from the revised estimation.

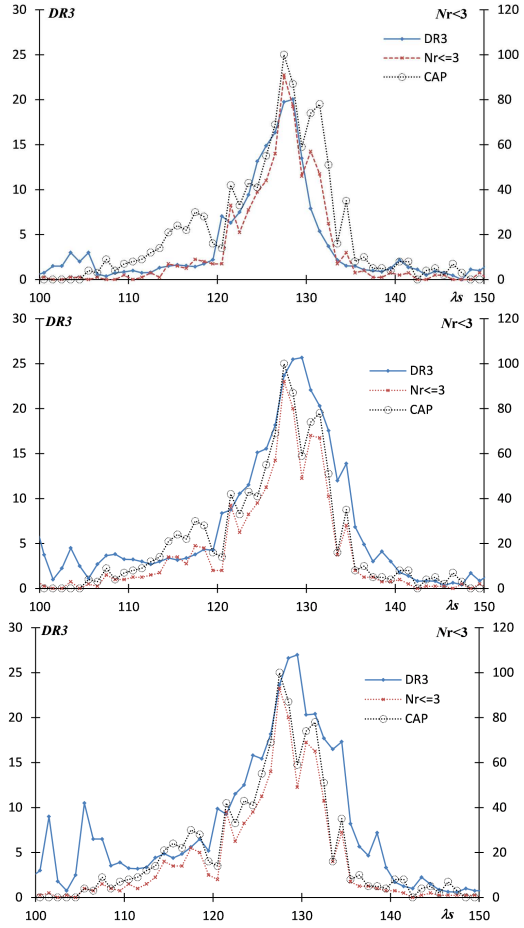

Figure 2 – The activity profiles exhibited by DR of CAP: (a) without a correction for the radiant shift, (b) from the first linear regression, i.e. 4th step, and (c) from the revised estimation (5th step).

(profile) can show the difference in the result of the 2nd and the 4th step. The radiant distribution becomes more compact and the profile wider because the counting area moves along with the radiant drift. We can, therefore, select the radiants in a smaller area and in wider time span to revise the radiant shift estimation. The revised linear regressions are computed for data 3° from the estimated center and the earlier and later 10 degrees from the selected λ_s in the 1st step.

2.5 Estimation of the profile by using the refined radiant estimation of the 4th step

We can re-calculate the radiant distribution and the profile from the refined estimation. The radiants concentrate close enough (Figure 1d) and the profile (Figure 2c) looks like that of the 4th step. Further recalculations show no significant improvement and the results of the 5th step can be accepted as final. The revised linear regression signifies the radiant shift given in Table 2, though this is only an example for the explanation.

3 Activity profiles of several example meteor showers

3.1 Geminids (GEM)

The GEM is a suitable example to check the DR method because the activity profile of GEM is well known from visual observations. Figure 3 shows the radiant distribution of GEM from the 2nd step. The distribution is almost round suggesting a small radiant shift. Figure 4a and 4b show the profiles after the 2nd and the 4th step. The two profiles are similar because of the small radiant shift of the GEM. We can use the profile of the 2nd step for such meteor showers. We recognize the curve of recorded meteors N3 is very similar to the visual one but both DR profiles (Figure 4a and 4b) are different from the former two in their slope. The profiles obtained from the DR seem to be widened but it is flattened in fact. We use the radiant density ratio within 3° to 3° to 6° from the center and, therefore, DR3 would be lowered when the shower radiant are spread over 3° from the center around the maximum (Figure 3). Figure 4c adds the DR10 profile calculated by using the outer range as 6° to 10° degrees instead of 3° to 6°İt is clear that the DR10 profile rises much higher than that of DR3, because the GEM spread radiants decrease rapidly with the distance from the center. We must be careful with DR3 profiles of major show-

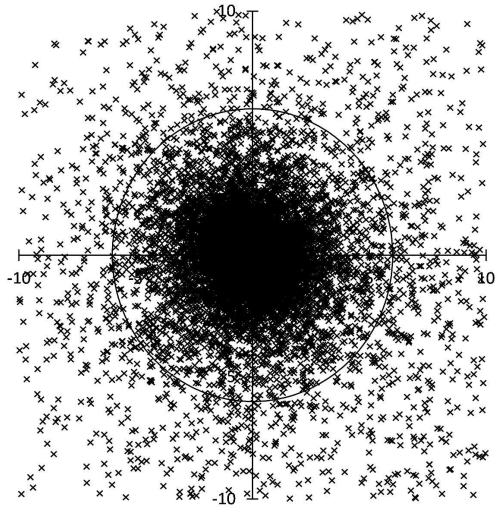

Figure 3 – The radiant distribution of GEM from the estimate of the first linear regression in $\lambda - \lambda_s, \beta$

Table 2 – Estimated radiant shift of the Capricornids after the 5th step.

λ_s [°]	105	110	115	120	125	130	135	140	145
$\lambda - \lambda_s$ [°]	187.3	185.4	183.5	181.6	179.7	177.7	175.8	173.9	172.0
β [°]	7.4	7.9	8.5	9.0	9.6	10.1	10.7	11.2	11.8
α [°]	292.8	295.8	298.8	301.8	304.7	307.5	310.4	313.2	315.9
δ [°]	−14.3	−13.3	−12.2	−11.0	−9.8	−8.5	−7.2	−5.9	−4.5
V_g [km/s]	26.7	25.7	24.6	23.6	22.6	21.6	20.5	19.5	18.5

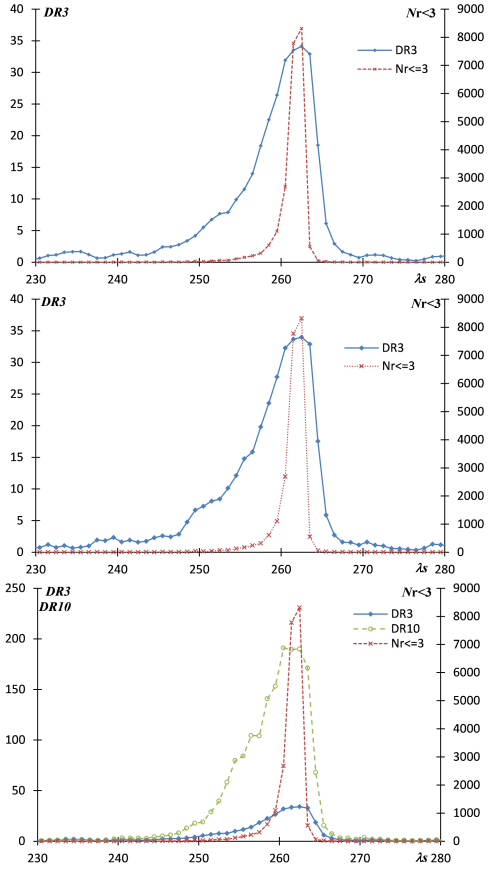

Figure 4 – The activity profiles expressed by the DR of GEM. (a) without correction for the radiant drift, (b) using a correction of the radiant drift after step 4, and (c) DR10 profile calculated by using the outer range of 6–10° instead of 3–6° for step 4.

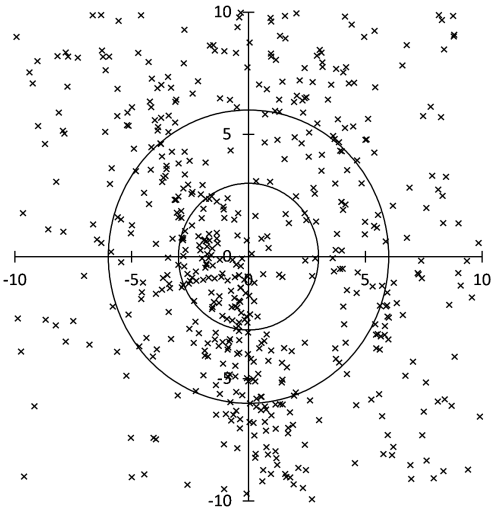

Figure 5 – The radiant distribution of KCG in $(\lambda - \lambda_s, \beta)$ without a correction for the radiant drift.

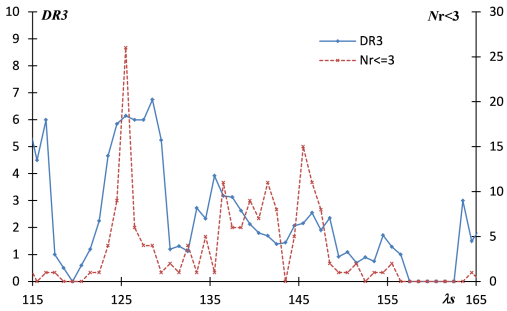

Figure 6 – The activity profiles expressed by DR of the KCG without a correction of the radiant drift.

ers, because DR3 might be lowered when the shower radiants widely scatter.

3.2 Kappa Cygnids (KCG)

We cannot derive reliable results for the KCG from the above stated processes only. The author studied the KCG in detail (Koseki, 2014) and showed that the KCG has two unique features: a periodicity of the activity of 7 years (Table 3) and an elongated radiant distribution (Figure 5). The appearance of the KCG in a peak year of the 7 years period is quite different from the average years. We have to analyze these two activities separately. It is noticeable that the median RP of the SD (the center of the figure) is apart from the elongated radiant distribution; the median RP is based on the regular years and the radiant concentration is from the peak year. If we treat them as one meteor shower, we cannot reach the real profile of the KCG. Figure 6 shows the unclear activity profile of compounded KCG. DR and N3 show that the activity peak occurs around $\lambda_s = 125°$ and the activity of the supposed KCG peak is lower than the former. The former activity coincides with the July gamma-Draconids (GDR). The results of the 4th step cannot show the clear improvement of course. We can reach the clear results only by taking into account the unique properties of KCG (see details Koseki, 2014).

3.3 Ursids (URS)

The URS does not show noticeable activity in regular years but yielded small outbursts several times (Table 4). In contrast to the KCG, the URS radiant distribution is ordinary and is surrounded by the background sporadic activity as usual (Figure 7). Figure 8 shows the profile of URS drawn from the result of the 2nd step. It is clear that the URS is active during only a week at most, probably recognizable a few days around the maximum. This short duration of URS causes difficulties for us to calculate the radiant shift and compels us to use the results of the 2nd step. We should be care-

Table 3 – Number of meteors originally classified as KCG in SonotaCo net.

Year	2007	2008	2009	2010	2011	2012
N	204	13	18	34	16	44

Year	2013	2014	2015	2016	2017	2018
N	54	140	21	32	18	43

Table 4 – Number of meteors originally classified as URS in SonotaCo net.

Year	2007	2008	2009	2010	2011	2012
N	10	32	69	62	99	16

Year	2013	2014	2015	2016	2017	2018
N	32	32	13	30	153	28

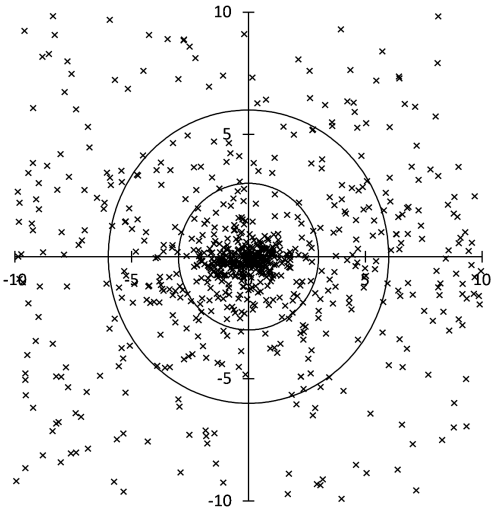

Figure 7 – The radiant distribution of the URS in $\lambda - \lambda_s, \beta$without correction for the radiant drift.

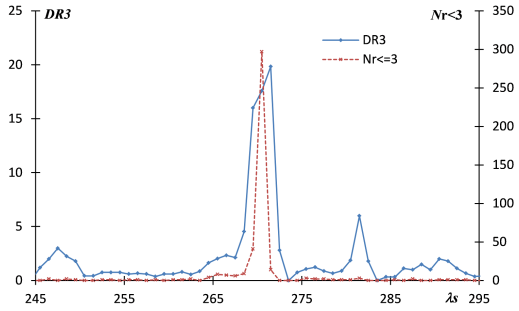

Figure 8 – The activity profiles expressed by DR of the URS without a correction for the radiant drift.

ful to classify a meteor as a member of URS because of the background sporadics, the fluctuation of the activity and the short duration.

3.4 Sigma Hydrids (HYD) and Eta Hydrids (EHY)

The HYD is only a minor shower for visual observers but is ranked high (Table 2 of Koseki, 2018) by video observations. The HYD seems to be rich in bright meteors. CMOR1 did not report HYD (Brown et al., 2008) and CMOR2 detects HYD barely (Brown et al., 2010). The preliminary result, that is, the 2nd step, shows the HYD's slow radiant motion:

$$\lambda - \lambda_s = -0.11107 * \lambda_s + 259.31$$

and

$$\beta = -0.00071 * \lambda_s - 16.21.$$

The radiant distribution in the 2nd step is already round (Figure 9) and the profile is clear enough (Figure 10). The HYD has neighbouring activity of the EHY (the left group of HYD in Figure 9) but HYD meteors are much more abundant than EHY and therefore it is not necessary to compensate the influence of the EHY – Figure 10 is not compensated for EHY activity. If we want to construct the DR profile of EHY, we need to exclude the influence of HYD. If we strictly use DR curves, the result is miserable (Figure 11a). Figure 11b shows the result when we do not count meteors on right side between 3° to 6° from the center of EHY. It is clear that the DR profile is not perfect but still useful by adopting

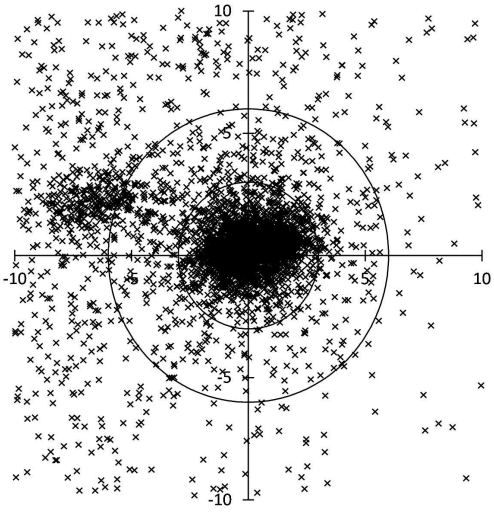

Figure 9 – The radiant distribution of HYD in ($\lambda - \lambda_s$, β) without a correction for the radiant shift.

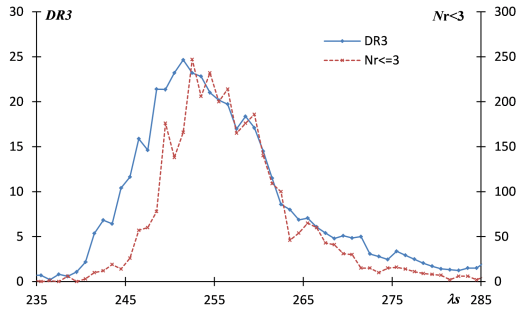

Figure 10 – The activity profiles exhibited by DR of HYD without a correction for the radiant shift.

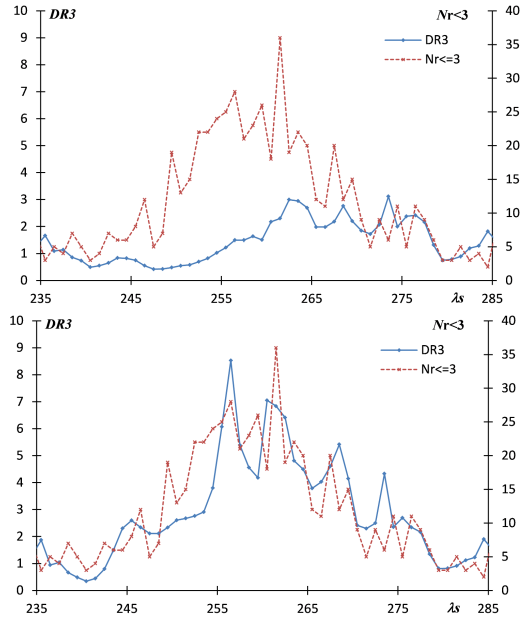

Figure 11 – The activity profiles exhibited by DR of EHY without a correction for the radiant shift. a: usual DR curve and b: excluding meteors right side between 3 to 6 degrees to avoid the influence by HYD.

the circumstances. We had better to draw the activity profile by N3 the meteor number within 3° from the center when we do not any compensation. If we use the meteor number as the index of the activity profile, including more distant meteors such as 5° leads us erroneous result because of the neighbour activity such as the HYD.

3.5 Andromedids (AND)

The author pointed out that a small crowd of radiants moves fast and passes through the 1872 Andromedid storm around $\lambda_s = 245°$ (Koseki, 2014). We can find the elongated radiant distribution from bottom left to top right at the 2nd step (Figure 12a). The radiant distribution is reduced to a small ellipse by the 4th step (Figure 12b) and by the 5th step the radiant distribution settles in a small circle (Figure 12c). This final step gives us a clear DR profile (Figure 13).

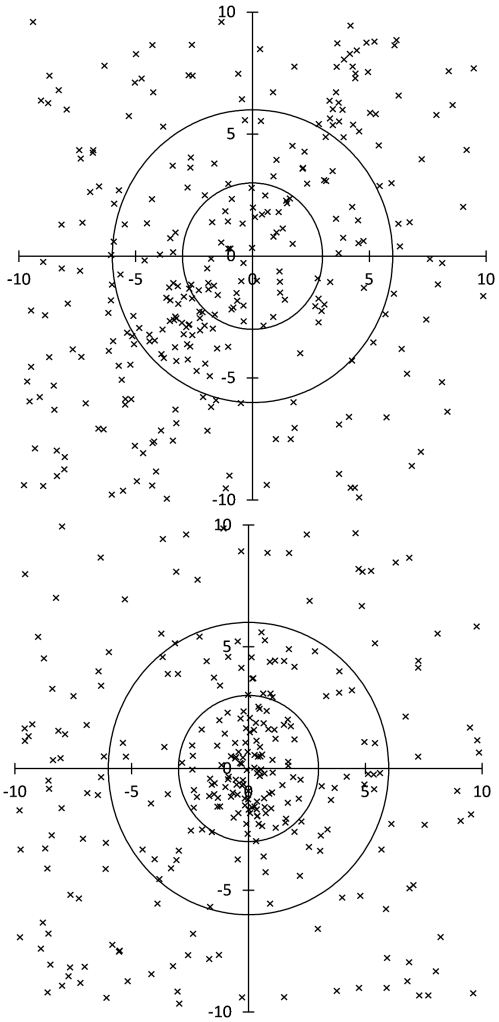

Figure 12 – The radiant distribution of AND in ($\lambda - \lambda_s$, β). a: without a correction for the radiant shift, b: by the estimation from the first linear regression and c: by the revised estimation.

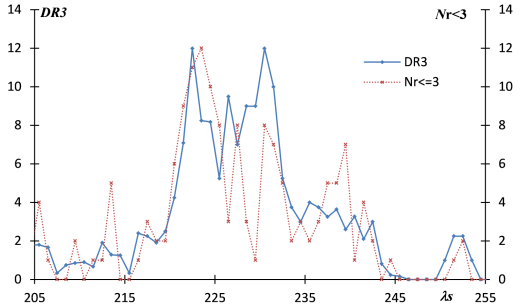

Figure 13 – DR activity profiles of the AND by the revised radiant estimation (the 5th step).

We can estimate the radiant shift by the final (5th) linear regression as shown in Table 5. The radiant seems to move toward historical "Bielids" radiant with λ_s and reach at it in accordance with λ_s of the "Great Andromedids". We can trace the procession from recent AND activity to the historical apparition again in this different procedure.

3.6 December Monocerotids (MON) and November Orionids (NOO)

Both meteor showers had been in confusion and called as "Monocerotids" in the 1970s because the radiant positions are close to one another and the activities seem to be continuous. It is necessary to compensate each influence to draw DR profiles as in the case of HYD and EHY. Figure 14a shows the radiant distribution of the MON centered at the median radiant point of MON within the set time span (see the step 1st). The NOO centered radiant distribution is shown in Figure 14b; the shapes of two showers are different from Figure 14a because the λ_s and the time span is different. It seems to be proper judging from the distribution that we calculate the DR of the MON using half the $3 < r < 6$ area of the left and right sides in case of the NOO.

We can obtain a profile of MON which is clear enough by the 4th step (Figure 15a), because the activity of the MON is stronger and the sporadic activity around the MON radiant is weaker than those of NOO. We need the revised linear regression for NOO but the result (Figure 15b) shows that this process cannot fully compensate the influence from MON. The curve of D10 becomes lower than D3 after $\lambda_s > 253°$ because of the disturbance from the MON. If we use the upper half of $3 < r < 6$ area for compensation, both DR curves would fluctuate largely because of sporadics and other

Table 5 – Estimated radiant shift of the Andromedids by the 5th step.

λ_s [°]	210	215	220	225	230	235	240	245	250
$\lambda - \lambda_s$ [°]	172.1	169.8	167.6	165.3	163.1	160.8	158.6	156.3	154.1
β [°]	10.9	13.3	15.8	18.2	20.7	23.1	25.6	28.0	30.5
α [°]	16.2	17.8	19.4	21.1	22.7	24.4	26.1	27.7	29.4
δ [°]	18.6	21.9	25.2	28.5	31.8	35.1	38.3	41.5	44.7
V_g [km/s]	20.9	19.9	19.0	18.1	17.1	16.2	15.2	14.3	13.3

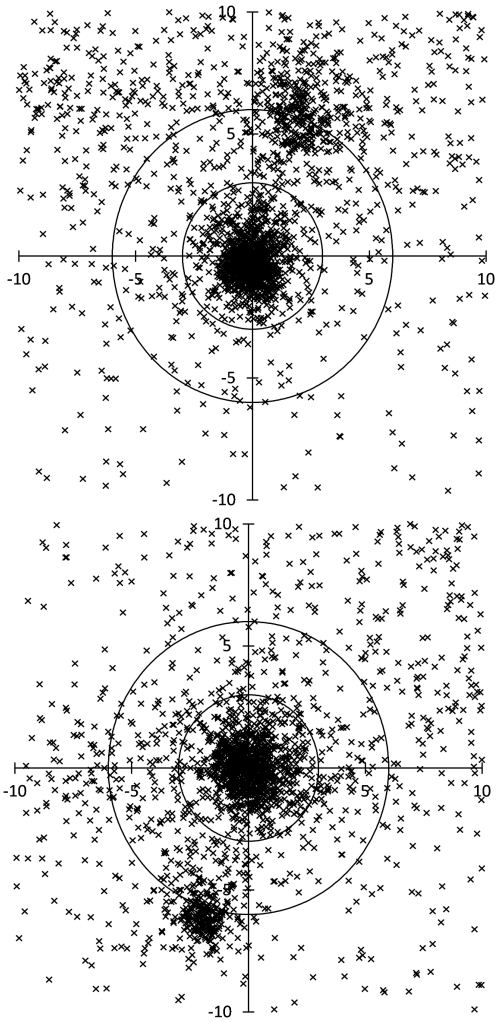

Figure 14 – The activity profiles exhibited by DR. a: MON by the estimation from the first linear regression using left side half area for $3 < r < 6$ and b: NOO by the revised radiant estimation (the 5th step) using right side half area for $3 < r < 6$.

activities. It is difficult to select the reference area, the area becomes smaller the meteor number also, the fluctuation of the radiant ratio larger.

The MON is a one of prominent meteor showers in video observations though not so in visual and radar observations. MON and NOO are rich in video data but high DR does not mean such meteor showers are prominent ones through the other views.

3.7 Leonis Minorids (LMI)

The LMI is another conspicuous meteor shower detected in video observations now and appeared formerly in photographic observations because of the low background activity. The LMI seems to be a stationary shower in $(\lambda - \lambda_s, \beta)$ coordinates and it is not necessary to take the radiant shift into consideration. Figure 16 shows the radiant distribution and Figure 17 the activity profile of the 2nd step. The peak DR of the LMI is higher than that of the NOO when we use the 2nd step result though the meteor number of LMI at the peak is smaller than that of the NOO. DR means the clearness of the meteor activity against the background activity and not the absolute activity level such as ZHR. DR can

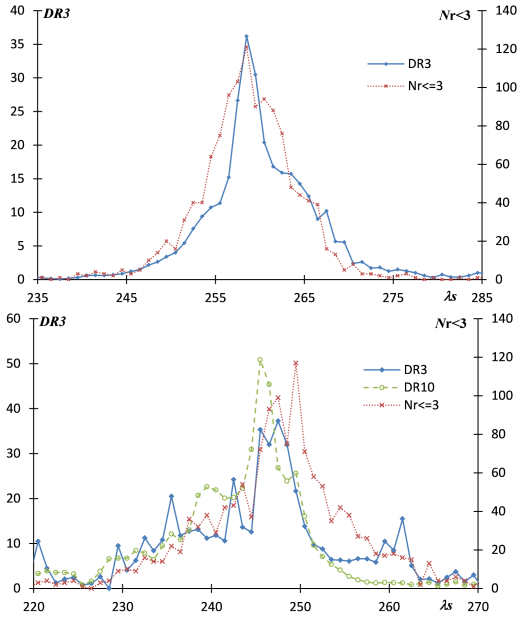

Figure 15 – The activity profiles exhibited by DR. a: MON by the estimation from the first linear regression using left side half area for $3 < r < 6$ and b: NOO by the revised radiant estimation (the 5th step) using right side half area for $3 < r < 6$.

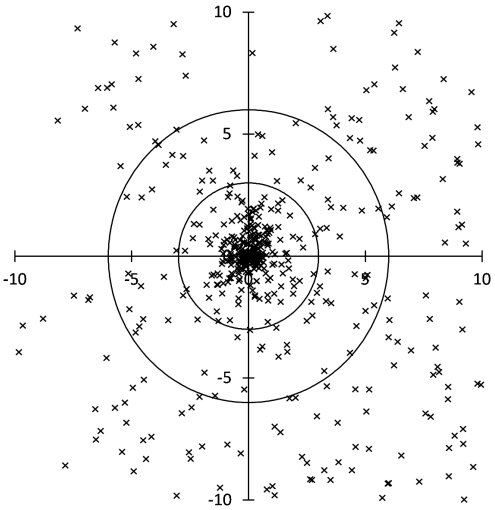

Figure 16 – The radiant distribution of LMI in $(\lambda - \lambda_s, \beta)$ without a correction for the radiant shift.

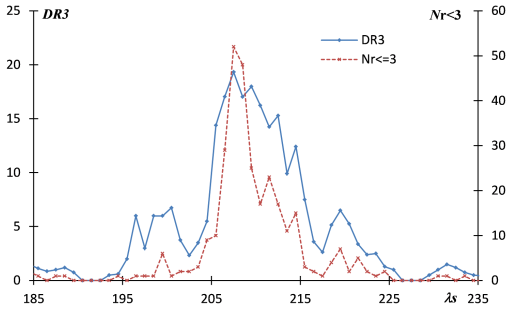

Figure 17 – The activity profiles exhibited by DR of LMI without a correction for the radiant shift.

make easy to see weak meteor activities but is affected by the neighbour radiant distributions.

3.8 Epsilon Geminids (EGE)

The EGE is a contrary example to the LMI: the EGE radiant is surrounded by very busy background activities composed not only of the (October-)Orionids (ORI: bottom right of Figure 18) but also of sporadics. Such background activities hinder us much in drawing the profile and it is necessary to revise the linear regression to the 5th step. Figure 18 shows that the EGE is almost buried in the background and the DR profile of the EGE does not signify the maximum even at the final step (Figure 19). The numbers of meteors within 3° from the center N3 are high but DRs suggest the activity is not high enough for visual observations. If EGE locates far from ORI and the background is busy, observers might feel difficulty to point out its activity center. It should be careful to classify a meteor to a specific meteor shower, visual observers who do not plot meteor paths cannot discriminate EGE from other activities. It seems to be adequate to discriminate meteors by the distance 3° from the radiant and not 5° degrees or more even if video and photographic observations.

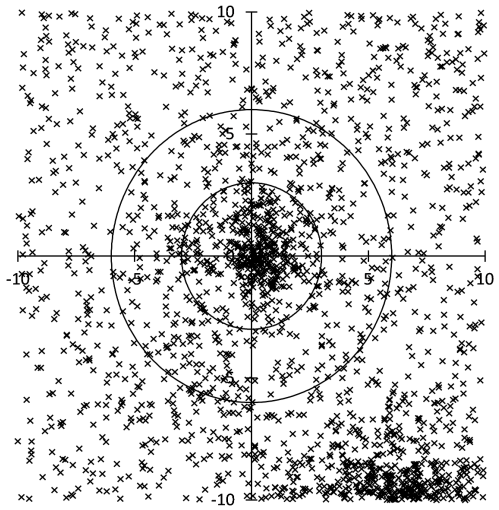

Figure 18 – The radiant distribution of EGE in $(\lambda - \lambda_s, \beta)$ by the revised estimation (5th step).

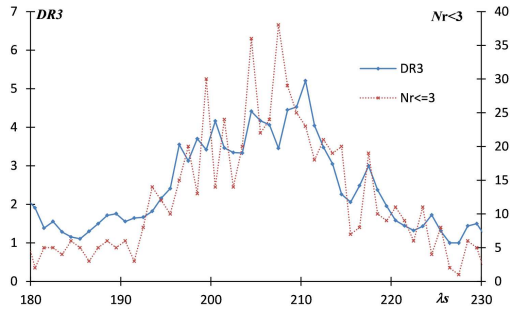

Figure 19 – The activity profiles exhibited by DR of EGE by the revised radiant estimation (the 5th step).

3.9 January Comae Berenicids (JCO)

The JCO is now on "working" status but McCrosky and Posen (1959) referred to the JCO as "Coma Berenicids" through photographic observations. The discovery of JCO was followed by the December Leonis Minorids (DLM; Cook et al., 1973) and the December Comae Berenicids (COM; Lindblad, 1971). DLM was indicated as association VII by Whipple (1954) and is recognizable clearly since then. The DLM is the heart of the COM complex though the name was replaced to COM in the SD now. The very first SD listed these three showers as concerning COM complex (Table 6). The radiant distribution shows the radiant concentration around the center (Figure 20) but the DR profile does not indicate a clear rise of DR towards the median λ_s (Figure 21). DR descends rightward, that is, decrease with time slowly. This descent starts at DLM and continues through COM to JCO and afterwards. The COM complex in the SD is very confused and the author pointed out that the COM complex is composed of three meteor showers: DLM, COM and JCO (Koseki, 2011). Table 7 shows the possible photographic meteors; the abbreviations refer to Koseki (2009). Photographic meteors are divided clearly into three groups

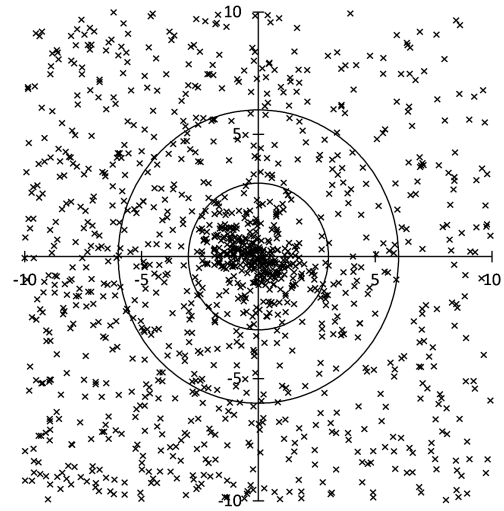

Figure 20 – The radiant distribution of JCO in $(\lambda - \lambda_s, \beta)$ without a correction for the radiant shift.

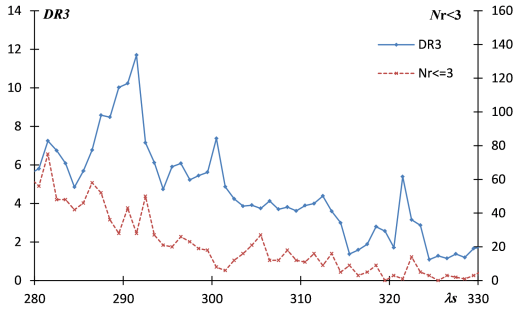

Figure 21 – The activity profiles exhibited by DR of JCO without a correction for the radiant shift.

Table 6 – Three meteor showers listed in the very first SD.

Code	λ_s	$\lambda - \lambda_s$	β	V_g [km/s]
DLM	262.°4	243.°2	21.°1	62.3
COM	274°	242.°7	20.°9	64
JCO	301°	240.°3	18.°9	63.9

Table 7 – The possible members of COM complex selected within 5° from each radiants of Table 6. The distance from the radiant shown in Table 6 are shown in the column r.

DLM Code	λ_s [°]	$\lambda - \lambda_s$ [°]	β [°]	V_g [km/s]	r [°]
H1-5988	262.7	244.2	21.7	59.4	1.1
H1-9559	260.7	243.3	19.5	67	1.7
H1-9593	260.7	243.7	22.9	62.4	1.8
H5-2578	261.6	243.9	22.9	65	1.9
H1-9802	264.7	245.1	21.8	60.3	1.9
H1-6027	264.7	245.9	22.1	62.7	2.8
D2-573287	268.2	246.3	22.3	57.4	3.2
H1-6038	265.7	247.5	21.0	60.5	4.1
COM Code	λ_s	$\lambda - \lambda_s$	β	V_g	r
H3-10012	284.3	242.7	20.0	63.75	0.8
H2-9948	283.2	243.7	20.7	63.5	0.9
D6-680103a	283.6	241.8	16.5	62.56	4.5
JCO Code	λ_s	$\lambda - \lambda_s$	β	V_g	r
H1-6243	297.7	240.2	18.5	58.5	0.5
H1-10075	293.7	241.5	19.5	65.9	1.3
D3-630215	302.7	241.8	19.3	63.9	1.5
H2-6264	299.7	242.3	19.4	64.7	2.0
H1-6332	303.7	239.7	20.8	62.9	2.0
H1-10083	293.7	242.8	19.0	64.8	2.4
H1-6191	295.7	237.2	17.4	57.4	3.3
H5-1918	300.5	236.7	20.9	63.6	3.9

by a dip of about 10° in λ_s. We understand that the JCO was not weaker than COM and its activity was distinguishable. It might be suggested the activity became weaker from then and would change in the future. We will study the contrary cases in the following sections.

3.10 July Pegasids (JPE)

Japanese observers are affected by the rainy season when the JPE is active. Figure 22 represents the radiant distribution of the JPE from EDMOND observations (Kornoš et al., 2014a, b); drawn by the 4th step because the JPE shows a clear radiant shift. The JPE is located in an area with high background similar to the COM complex and the small group of radiants on

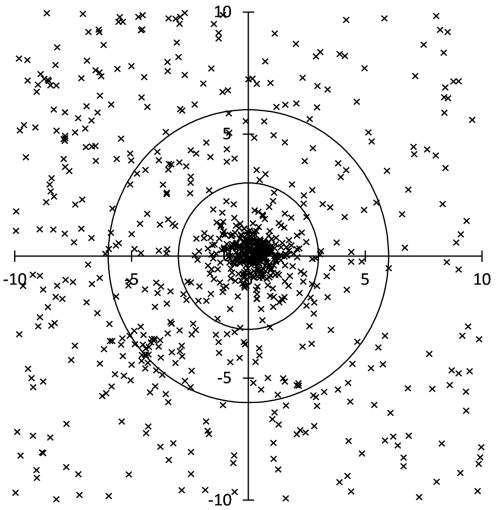

Figure 22 – The radiant distribution of JPE in ($\lambda - \lambda_s$, β) corrected by the 4th step by EDMOND observations.

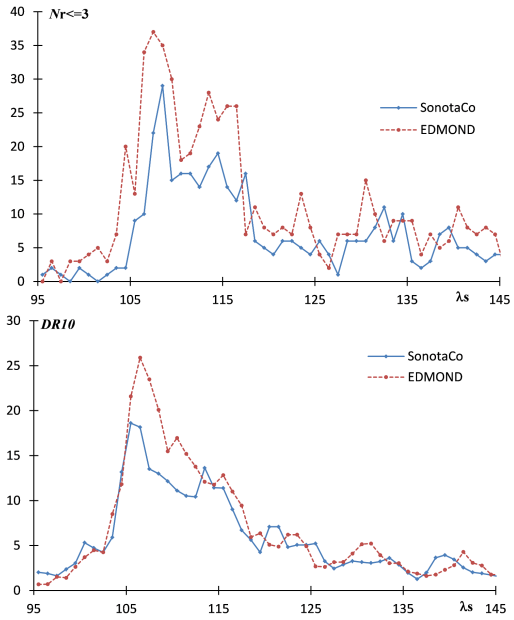

Figure 23 – The activity profiles of JPE compared EDMOND results with SonotaCo's. a: recorded meteor number within 3° from the center (N3) and b: DR10.

the lower left edge of the 6° circle might be 0829JSP00. But it seems that there is only the sporadic background around the JPE radiant and so we use the outer area between 6° and 10° instead of 3° to 6° in order to get clear profile. Figure 23a and 23b give the activity profiles of the JPE by N3 and DR10 comparing SonotaCo's results. N3s of SonotaCo are lower in almost whole period than EDMOND's (Figure 23a) because the former are restricted by the rainy season and the both the EDMOND and SonotaCo results fluctuate widely. DR10 curves of the both are similar and smooth though SonotaCo's drops fast after the peak (Figure 23b). This difference is not clear but the rich sporadic activity including possible 0829JSP00 might explain the discrepancy. The rapid rise and slow descend of the profile are the peculiarity of JPE and resemble COM complex; the latter part might be formed up with some components also. When there is no active shower within the period, we would be better to use the outer range as the reference area. DR values in the ordinary case of 3° to 6° are lowered when the shower radiants are spread widely as describing in the section of GEM, DR values derived by using the outer area would be higher than the former in such cases. DR shows the relative strength of the activity and not the absolute one and the comparison of DR obtained by two reference areas is meaningless.

It is interesting that photographic observations have no certain JPE meteors. The only possible candidates are: O1-45 ($\lambda_s = 119\overset{\circ}{.}3$), H5-1735 ($\lambda_s = 127\overset{\circ}{.}5$), O1–4 ($\lambda_s = 128\overset{\circ}{.}0$). All three meteors locate more than 3° from the center and seem to be too late. It is suggested that the JPE is the younger sister of the COM complex; Coma Berenices means "Berenice's Hair" in Latin and refers to Queen Berenice II of Egypt in the other world. But, Medusa and the bereaved immortal sisters Stheno and Euryale are wandering about the world. We now find out the traces of them as Hairs of Medusas Sisters;

JPE and SPE are located very near the COM radiant in $(\lambda - \lambda_s, \beta)$, although not the period of activity of course.

3.11 September epsilon Perseids (SPE)

The radiant distribution (Figure 24) and the profile (Figure 25) both are compact; a small group lower left between two circles might be 0874PXS00. Almost all SPE radiants are located within 3° from the center, though Figure 24 is constructed in the period of $\lambda_s = 158° - 178°$. SPE radiant seems to shift only slightly and it is negligible for the DR calculation. The duration of SPE is short – a few days around the maximum even if taking DR > 2 into consideration $\lambda_s = 160° - 175°$ at the most. The DR curve is wider than that of meteor numbers, because DR is calculated for a 3° λ_s-bin and shows the relative activity level to the reference area. We can find photographic observations of SPE within 5° from the center (Table 8). However, it is necessary to note that C4-21951 was recorded in 1959 and H6-39745A, H6-39742B and O4-504 were observed in 1967. There is no certain SPE in the Harvard 1952–54 survey. H1-4518 and H1-4558 are within 3° but beyond the activity duration in λ_s and only H1-4408 is a possible member. The SPE might become active or change its activity widely (Table 9), and is suggested the youngest sister of the three.

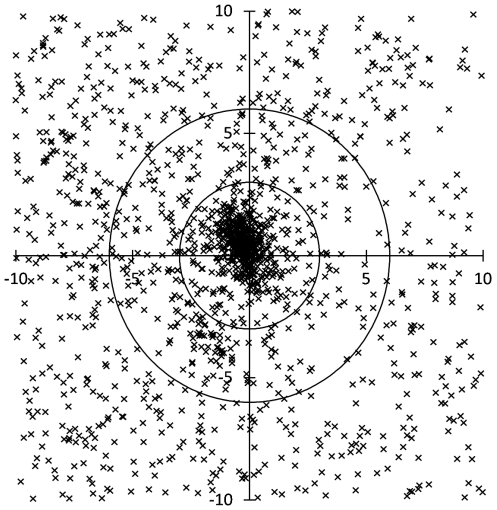

Figure 24 – The radiant distribution of SPE in $(\lambda - \lambda_s, \beta)$ without a correction for the radiant shift.

Table 8 – Possible members of SPE selected within 5° from the median radiant of the SPE. The distance from the radiant shown in Table 6 are shown in the column r.

Code	λ_s [°]	$\lambda - \lambda_s$ [°]	β [°]	V_g [km/s]	r [°]
H6-39745A	168.7	249.5	20.5	65.3	0.7
H6-39742B	166.7	249.3	19.3	66.5	1.2
C4-21951	166.1	250.0	21.0	64.59	1.3
H1-4518	177.7	250.1	19.8	66.8	1.4
H1-4558	182.7	246.1	20.7	66.4	2.5
O4-504	169.1	251.9	19.3	66.72	3.1
H1-4408	174.7	252.1	19.0	69.7	3.4

Table 9 – Number of meteors originally classified as SPE in SonotaCo net.

Year	2007	2008	2009	2010	2011	2012
N	37	87	116	132	121	143

Year	2013	2014	2015	2016	2017	2018
N	95	68	41	38	61	42

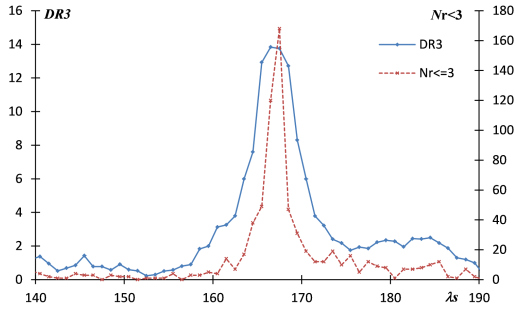

Figure 25 – The activity profiles exhibited by DR of SPE without a correction for the radiant shift.

3.12 Zeta Cassiopeiids (ZCS)

The ZCS has been doubted as the precursor of the Perseids (PER) and is listed as "working" in the SD. The radiant distribution is constructed in the period of $\lambda_s = 102.^{\circ}3 - 122.^{\circ}3$ and, therefore, the radiants of early PER contaminate the bottom left (Figure 26). The radiant of ZCS moves lower left and that of PER is stationary in $(\lambda - \lambda_s, \beta)$ coordinates (Koseki, 2018); the later ZCS is difficult to distinguish from the early PER. But the author wrote that ZCS is the independent activity clearly (Koseki, 2018), because their radiants are quite distinguishable even taking the radiant drift into account. The activity profiles (DR curves) of Figure 27a and 27b exhibit the separate and enough high peak of ZCS against PER. Figure 27b shows the complexity of the two activities; the meteor numbers within 3° N3 and DR10 increase rapidly with time after $\lambda_s > 116°$, because the radiant drift is taken into account and, therefore, the influence of PER increases.

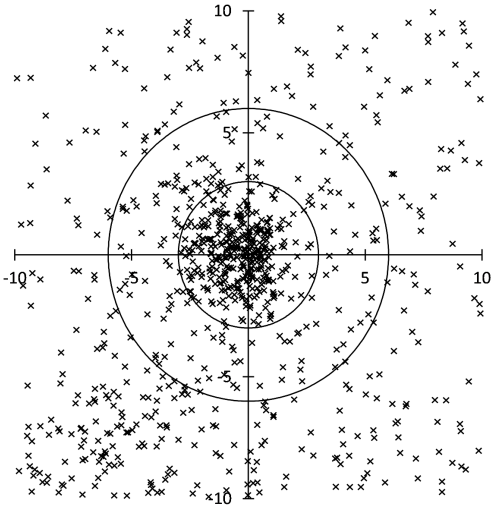

Figure 26 – The radiant distribution of ZCS in $(\lambda - \lambda_s, \beta)$ corrected by the 4th step.

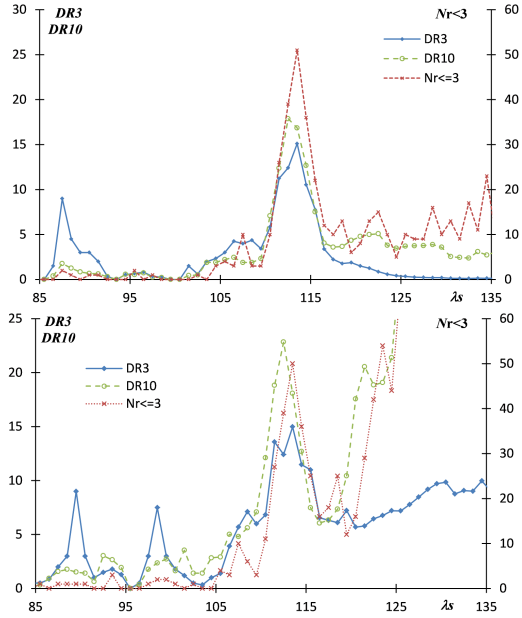

Figure 27 – The activity profiles exhibited by DR of ZCS. a: without a correction for the radiant shift and b: using a correction of the radiant shift by the 4th step.

DR3 of Figure 27a is affected only little by PER and shows a smooth descent; if we want to take a look at the profile of the ZCS, it would be better to use Figure 27a. This paper provides an additional proof to the independence of ZCS activity from the DR profile, even Figure 27b shows the independent peak of ZCS activity.

4 Discussion

Radiant positions should be expressed by the sun centered ecliptic coordinates $(\lambda - \lambda_s, \beta)$. It is not necessary to consider the radiant drift when we use this coordinate mostly except for the case detected a swift drift. We have calculated DRs using the 5th step, that is, computation of the revised radiant drift; but it is not necessary to calculate the radiant drift in many cases except for Andromedids, this is the only case necessary to carry out the 5th step. We can derive fine views of minor showers using the DR even if a nearby shower overlaps them. Respective examples are EHY, EGE and NOO. The DR gives the detectability of a meteor shower activity and works well especially for weak showers and those which are not yet well understood. The author applied the method to some weak activities and obtained refined results (Koseki, 2019a). The DR shows the relative activity against the surrounding ones. This way we do not obtain an absolute activity measure such as the ZHR but many observational deviations are cancelled out. In some cases it is necessary to modify the DR: if a stronger shower occurs within 6° or there are scarce radiant points in the reference area. The reference area could be modified to the side opposite to the obstacle or to the range of 6° to 10° or farther instead of 3° to 6°.

We could not show clear activity profiles for two showers: the KCG and JCO are unique cases and require individual further investigation. The KCG has a clear periodic nature and its characteristics vary considerably between the maximum years and the regular or average years. The JCO is a member of the COM complex and the distinction between its components is very difficult. It is necessary to synthesize the studies for such activities considering history, orbit, origin etc. including the DR.

5 Conclusions

1. The sun centered coordinates $(\lambda - \lambda_s, \beta)$ are useful to study meteor activity. The radiant shifts become negligible in many cases.

2. The radiant density ratio of the central 3 degrees to the ring between 3° and 6° (DR) is a good tool to characterize a meteor shower activity profile.

3. The DR shows the relative activity of the shower to the background and excludes observational bias to a large extent.

4. DR is sufficient to confirm a meteor shower activity, but it is better to adjust the outer limit of the reference area for a more exact profile.

References

Brown P., Weryk R. J., Wong D. K., and Jones J. (2008). "A meteoroid stream survey using the Canadian Meteor Orbit Radar. I. Methodology and radiant catalogue". *Icarus*, **195**, 317–339.

Brown P., Wong D. K., Weryk R. J., and Wiegert P. (2010). "A meteoroid stream survey using the Canadian Meteor Orbit Radar. II. Identification of minor showers using a 3D wavelet transform". *Icarus*, **207**, 66–81.

Cook A. F., Lindblad B. A., Marsden B. G., McCrosky R. E., and Posen A. (1973). "Yet another stream search among 2401 photographic meteors". *Smithsonian Contr. Astrophys.*, **15**, 1–5.

IAU MDC (2018). "Meteor Data Center". `https://www.ta3.sk/IAUC22DB/MDC2007/` .

Kornoš L., Koukal J., Piffl R., and Tóth J. (2014a). "EDMOND meteor database". In Gyssens M., Roggemans P., and Zoladek P., editors, *Proc. IMC Poznan, Poland, Aug. 22-25, 2013*. IMO, pages 23–25.

Kornoš L., Matlovic P., Rudawska R., Tóth J., Hajduková, M. J., Koukal J., and Piffl R. (2014b). "Confirmation and characterization of IAU temporary meteor showers in EDMOND database". In Jopek T. J., Rietmeijer F. J. M., Watanabe J., and Williams I. P., editors, *Proc. of the Meteoroids 2013 Conference, A.M. University, Poznan, Poland, Aug. 26-30, 2013*. A.M. University, Poznan, pages 225–233.

Koseki M. (2011). "Coma Berenicids and related activities". *WGN, Journal of the IMO*, **39:6**, 159–166.

Koseki M. (2014). "Various meteor scenes II: Cygnid-Draconid Complex (κ-Cygnids)". *WGN, Journal of the IMO*, **42:5**, 1.

Koseki M. (2015). "Various meteor scenes III: Recurrent showers and some minor showers". *WGN, Journal of the IMO*, **43:1**, 14–27.

Koseki M. (2018). "Different definitions make a meteor shower distorted—the views from SonotaCo net and CAMS". *WGN, Journal of the IMO*, **46:4**, 119–135.

Koseki M. (2019a). "Legendary meteor showers: studies on Harvard photographic results". *WGN, Journal of the IMO*, **47:5**, 139–150.

Koseki M. (2019b). "Showers of the IAU Meteor Data Center in the video data of SonotaCo: a simple and clear criterion for grading meteor showers". *WGN, Journal of the IMO*, **47:1**, 7–17.

Lindblad B. A. (1971). "Meteor streams". *Space Research*, **XI**, 287–297.

McCrosky R. E. and Posen A. (1959). "New photographic meteor shower". *Astron. J.*, **64**, 25–27.

SonotaCo (2009). "A meteor shower catalog based on video observations in 2007-2008". *WGN, Journal of the IMO*, **37**, 55–62. see also "SonotaCo Network Simultaneously Observed Meteor Data Sets": `http://sonotaco.jp/doc/SNM/`.

Whipple F. L. (1954). "Photographic meteor orbits and their distribution in space". *Astronomical Journal*, **59**, 201–217.

Handling Editor: Jürgen Rendtel

On a possible recurring feature in the Geminid stream

Jürgen Rendtel [1]

The analysis of visual and video data of the 2018 Geminid return allowed to study particularly the ascent towards the maximum ZHR of 150 on December 14 close to 14^h UT ($\lambda_\odot = 262\overset{\circ}{.}2$ to $262\overset{\circ}{.}3$). During the ascent, we found a deep "dip" in two independent data sets on December 14, 04^h UT ($\lambda_\odot = 261\overset{\circ}{.}85$) when the ZHR dropped from an early sub-peak (ZHR above 100) to 70, followed by a steep increase towards the main peak. Previous analyses of the shower activity did not show annually recurring features. Data from returns back to 1997 which are separated by roughly 5 Geminid orbital periods, i.e. 7 years, yielded hints at a ZHR depletion at the position of the 2018 dip.

Received 2019 November 21

1 Introduction

The Geminid shower is observed regularly because of its high rates (peak ZHR ≈ 150) and the long duration (FWHM ≥ 24 hours) of its maximum. Further, the radiant position is favourable for observers on both hemispheres, therefore a large amount of data can be collected which often allows us to compose a continuous data set.

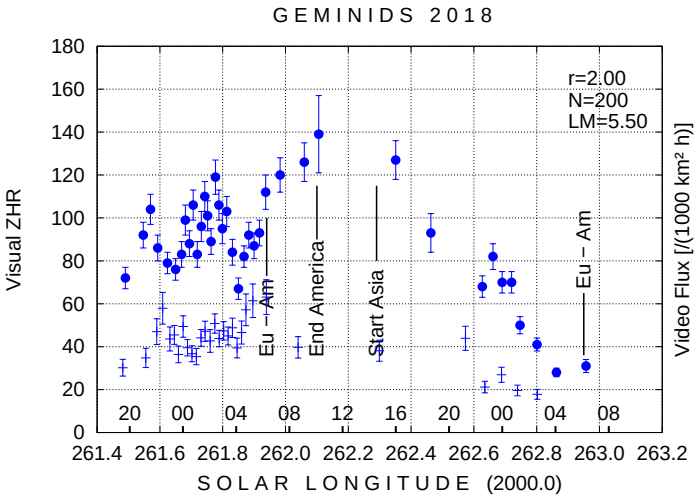

Figure 1 – Overview of the Geminid peak activity 2018 as observed visually (dots) and by video (crosses), setting population index $r = 2.00$ for the entire period. The time is given on the abscissa, starting December 13, 19^hUT and ending December 15, 04^hUT. For this overview we set $r = 2.00$ for both the visual and video data. The visual data have a minimum number of N=200 per bin and a limiting magnitude (LM) of 5.50 or better. The minimum number of video meteors is 60 per bin (using the temporary database of the IMO Video Meteor Network). The vertical lines mark the end / start of observing periods in different regions worldwide.

Analyses of the 2018 return have been prepared by Miskotte (2019) and Rendtel (2020), both mentioning in some detail the obvious "dip" in the ascending part of the profile centered at December 14, 04^h UT ($\lambda_\odot = 261\overset{\circ}{.}85$). This is in the middle of continuous observation runs for many observers in Europe and therefore is not subject to effects which might arise from combining different data sets. First, we show the Geminid maximum profile (Figure 1) as calculated by Rendtel (2020).

2 Ascent to the Geminid maximum 2018

A striking feature occurs in the ascending branch of the ZHR and flux density curve (Figure 1). After an early maximum on December 14 close to 03^h UT (at $\lambda_\odot = 261\overset{\circ}{.}78$) the visual ZHR decreases by 30% within ≈ 1 hour. Seen from the observers' perspective, the section of the profile is better described as a deep dip in the ascent towards the actual peak. Many European observers had the impression that the Earth moved into an "empty region" of the stream. This happened around the time of the highest radiant elevation, i.e. constant observing conditions. A ZHR decrease from 110 to 70 is striking as is the rapid increase to over 120 after that.

The dip in the ZHR and flux density profiles follows the above mentioned early maximum by just one hour and it centered on December 14, 04^h UT ($\lambda_\odot = 261\overset{\circ}{.}85$). Such a local minimum was not detected in the previous return (Figure 2 for the Geminids of 2017); see

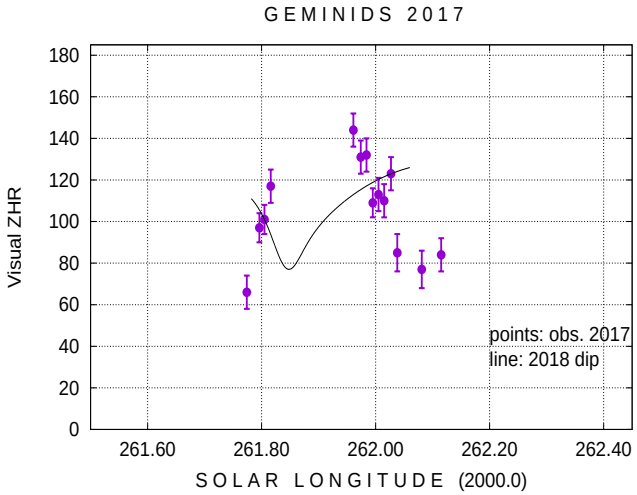

Figure 2 – Visual ZHR of the ascending branch of the Geminids in 2017 – i.e. the preceding return – for the interval around the 2018 minimum ($\lambda_\odot = 261\overset{\circ}{.}85$). The thin line shows a spline fit of the ZHR data during the dip found in 2018.

[1]Leibniz-Institut für Astrophysik, An der Sternwarte 16, 14480 Potsdam, Germany
and International Meteor Organization, Eschenweg 16, 14476 Potsdam, Germany.
Email: jrendtel@web.de

IMO bibcode WGN-476-rendtel-geminids
NASA-ADS bibcode 2019JIMO...47..180R

also Miskotte (2019). Attempts were also made to find sub-structures in the stream and to follow them over longer periods (Rendtel, 2004), with limited success. We want to emphasize that the ZHR and the video flux density graphs during the 2018 maximum profile confirm each other: the dip position coincides within 0.°01 (see Table 1) although the depth of the flux density decrease is less pronounced than in the visual data.

3 Relation to the meteoroid stream

Since the Geminid stream is close to the Sun, it seems unlikely to find permanent structures like dust trails in long period streams. The Geminid meteoroids are obviously on orbits which are very close to the parent 3200 Phaethon. The semi major axes calculated from video meteor data (Hajduková Jr. et al., 2017) are between 1.28 and 1.35 au; the current Phaethon orbit has $a = 1.271$ au. Hence the orbital periods are 1.433 years for Phaethon and 1.44–1.58 years for the Geminid meteoroids. This fits with a theoretical argument that the radiation pressure gradually increases the orbital period of the meteoroids (Kinsman & Asher, 2017). According to the numerical model of the Geminid stream of Ryabova (2016), despite the gravitational and non-gravitational perturbations, the meteoroids remain close to the parent and layers occur in the stream. As a consequence of the similarity of the orbits of Phaethon and the meteoroids, any *annual* recurring structure in the Geminid stream would imply that meteoroids extend over almost the entire orbit. If we assume particle concentrations of limited spatial extension along the orbit, these would *return only on some occasions*. However, the probability might be higher to find encounters after 7 years. During this time the Geminid meteoroids have completed a little over 5 orbits, close to a commensurability.

4 Searching for structures 1996–2018

As a first check, we looked into the VMDB data for 2011. The result is shown in Figure 3. Unfortunately, there is only a single visual ZHR value at $09^{h}20^{m}$ UT ($\lambda_{\odot} = 261.°85$). Plotting the 2018 dip-section into data shown in Figure 3 it fits surprisingly well into the 2011 data, but a single data point does not prove anything.

However, the case gets more weight when looking at the 2004 ZHR – another 7 years back (and differing more from 5 Geminid orbital periods). The 2018 dip-profile (thin line in Figure 4) fits surprisingly well here, although requiring a slight shift of $-0.°03 \pm 0.°025$ (i.e less than 1 hour) in time – perhaps in indication that the 7:5 relation is not perfectly fulfilled. Since the 2004 profile looks well covered, we check the situation with 2003 (Figure 5). This is a year ahead of the obviously well established dip in 2004, and repeats to some extent the 2017 – 2018 situation. The 2003 profile has no dip at $\lambda_{\odot} = 261.°85$, but a rate depletion 0.°10 (more than 2.5 hours) ahead of the 2018 position.

We extended our search by another 7 years backwards to 1997 (Figure 6), now three times the period. Here, the 2018 dip-profile coincides with a lower value

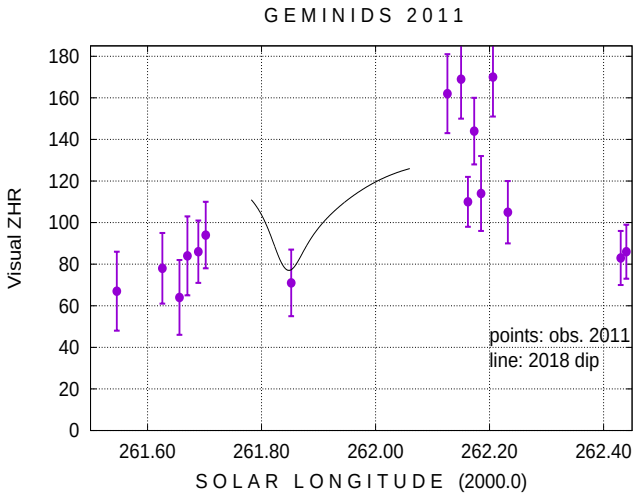

Figure 3 – Visual ZHR of the ascending branch of the Geminids in 2011 (about 5 orbital periods of the Geminids back from 2018) for the interval around the minimum at $\lambda_{\odot} = 261.°85$ found in 2018. The thin line shows the ZHR data of the dip found in 2018.

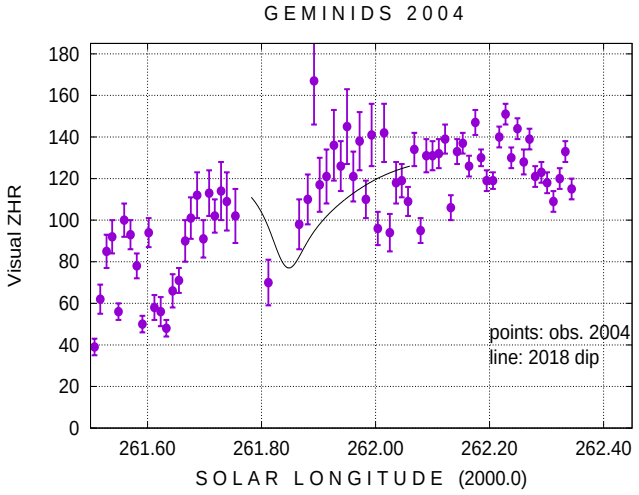

Figure 4 – Visual ZHR of the ascending branch of the Geminids in 2004 (another 5 orbital periods of the Geminids back) for the interval around the 2018 minimum ($\lambda_{\odot} = 261.°85$). The thin line shows the ZHR data of the dip found in 2018. This dip is also clearly visible in Figures 3 and 5 of Arlt & Rendtel (2006). It coincides with a period with a very low population index $r = 1.63$ (Figure 4 in that paper).

(which occurs 0.°01 behind the 2018 position). We also see that the general activity level in 2018 is higher than in 1997, a trend which fits the model and recent verification (Ryabova & Rendtel, 2018).

Eventually we checked data of all Geminid returns back to 1996 and also the available video flux data (2011–2018). We noted all returns which showed a dip in the vicinity of $\lambda_{\odot} = 261.°85$ ($\pm 0.°16$, i.e. 4 hours). The results are listed in Table 1. While a few ZHR/flux profiles showed a minimum very close to the 2018 position, we found further profiles which also show a dip in the ascending branch. Whether these can be related to the supposed recurring dip must remain open from our data. It might well be that the Earth encounters inhomogeneous regions when approaching the stream's

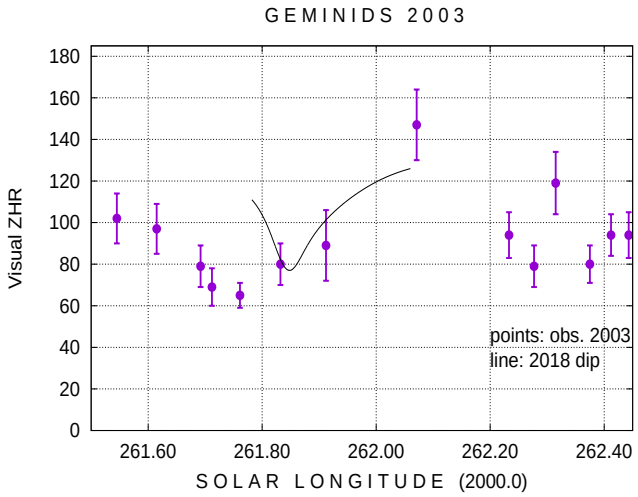

Figure 5 – Visual ZHR of the ascending branch of the Geminids in 2003 – one year before another 5 orbital periods of the Geminids back for the interval around the 2018 minimum ($\lambda_\odot = 261\overset{\circ}{.}85$). The thin line shows the ZHR data of the dip found in 2018. This repeats (approximately) the situation 2017 – 2018, also a year ahead of the deep 2018 dip.

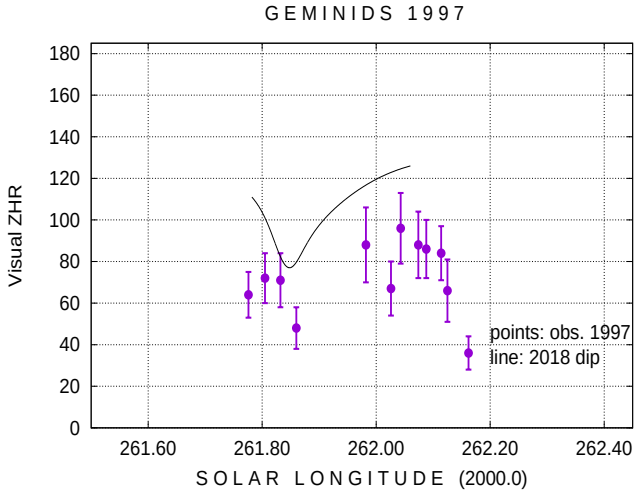

Figure 6 – Visual ZHR of the ascending branch of the Geminids in 1997 (another 5 orbital periods of the Geminids back) for the interval around the 2018 minimum ($\lambda_\odot = 261\overset{\circ}{.}85$). The thin line shows the ZHR data of the dip found in 2018.

central part. In Figure 7 we summarize the findings from the period 1996–2018. The zero line marks the position of the clear 2018 dip and the shift gives the difference of local minima found nearby. Deviations are less defined from one return to another. Hence the shift is rather an indication whether we see a dip and how much it is different in solar longitude from the 2018 position. We think that dips further away than $0\overset{\circ}{.}08$ (≈ 2 hours) have little to do with the supposed structure (referring to a linear distance along the Earth's encounter path of more than 250 000 kilometres). In Figure 7, the open squares mark the 7-year steps backwards from 2018 (the respective ZHRs are also plotted as large symbols). Empty dots describe uncertain data, which may concern the number of data points or the fit of any dip in the vicinity of the suspected position. The available

Table 1 – Positions of (potential) dips in the vicinity of $\lambda_\odot = 261\overset{\circ}{.}85$ found in visual and video data. "No data" indicates that there is no data in the interval about $0\overset{\circ}{.}2$ around the suspected dip position. ([1]) – few data, hence less defined profile; ([2]) – uncertain whether there is a dip; ([3]) – far off the reference position. The FluxViewer allows to access video data back to 2011.

Year	Deviation from $\lambda_\odot = 261\overset{\circ}{.}85$, [°]	
	Visual	Video
2018	(0)	-0.01 ± 0.004
2017	no dip	$+0.09 \pm 0.01$
2016	no data	no data
2015	$+0.07 \pm 0.03$	-0.08 ± 0.03
2014	$+0.02 \pm 0.005$	-0.01 ± 0.008
2013	$+0.04 \pm 0.02$	$+0.06 \pm 0.006$
2012	-0.09 ± 0.02	no data
2011	0.0 ± 0.15	no data
2010	no dip	
2009	-0.04 ± 0.04	
2008	no data	
2007	0.0 ± 0.05 ([1])	
2006	-0.02 ± 0.014	
2005	$+0.015 \pm 0.015$	
2004	-0.03 ± 0.025	
2003	-0.10 ± 0.04 ([1])	
2002	$+0.01 \pm 0.02$ ([2])	
2001	0.0 ± 0.03	
2000	no data	
1999	$+0.08 \pm 0.02$	
1998	no data	
1997	$+0.01 \pm 0.02$	
1996	-0.14 ± 0.08 ([3])	

video flux density values are plotted as (black) squares. Dip features which are more than $0\overset{\circ}{.}08$ (2 hours) away from the "reference position" are less likely associated with a flux density structure in the stream.

5 Conclusions

The remarkable dip in the 2018 profile on December 14, 04^{h} UT ($\lambda_\odot = 261\overset{\circ}{.}85$) in visual ZHR and video flux density data is located in the ascending branch of the profile. We first considered it a side effect, and the fact that it was not observed in a similar way in 2017 was not a surprise. Assuming a density structure in the Geminid stream, it would require a commensurable period to meet it again. Hence we looked into the data of returns which are multiples of 7 years back. Although the 2011 data point appears of low significance, the 2004 profile is very similar to 2018 with a dip from ZHR = 110 to 70 (Figure 4), while the 1997 data fits but is less convincing (Figure 6). Besides the dips found in the mentioned years, there are further dips e.g. in 2005 and 2006 – following the well visible 2004 dip. The variations discussed here are not found in data obtained from radio forward scatter observations (a respective profile is shown by Rendtel (2020)).

Both, the ascent to and the descent from the Geminid maximum show fluctuations at each return, indicating a kind of filamentary structure in the stream. The

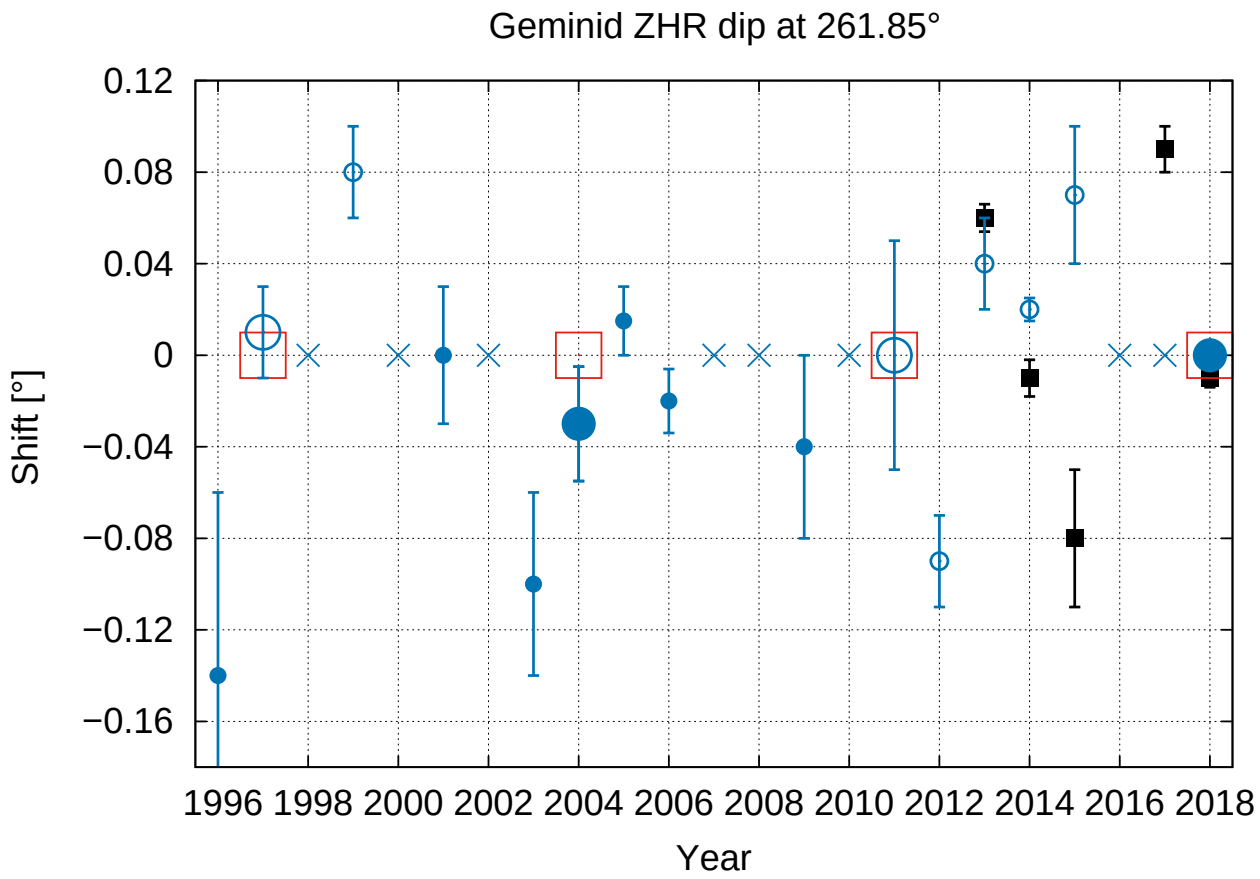

Figure 7 – Deviation of dip positions found in the annual ZHR / video flux density profiles close to $\lambda_\odot = 261\overset{\circ}{.}85$ which is the position of the dip observed in 2018 (zero line here). Dots refer to dips occurring in the visual ZHR data, where large dots – values for the 7-year difference, small dots – reliable dips in other years, empty dots – from incomplete profiles. Boxes mark the respective data from video observations. Large open squares mark the 7-year period. Crosses indicate years with no visual data closer than $0\overset{\circ}{.}2$ to the reference position. $\Delta\lambda_\odot = 0\overset{\circ}{.}04$ corresponds to ≈ 1 hour; a negative shift indicates an earlier position.

width may be roughly estimated from the typical duration of sub-peaks (about 1 hour, i.e. of the order of 10^5 km). Their extension along the orbit cannot be accessed from ground based observations. If we may trace such structures for several Geminid orbital periods, we may estimate the length along the stream's orbit.

Sub-maxima and dips require confirmation by various data sets before it may be assumed that these are regions in the Geminid stream with higher or lower spatial number density, which then needs to be explained by theoretical modelling.

References

Arlt R. and Rendtel J. (2006). "The activity of the 2004 Geminid meteor shower from global visual observations". *MNRAS*, **367**, 1721–1726.

Hajduková Jr. M., Koten P., Kornoš L., and Tóth J. (2017). "Meteoroid orbits from video meteors. the case of the Geminid stream". *Planetary and Space Sci.*, **143**, 89–98.

Kinsman J. H. and Asher D. J. (2017). "Evidence of Eta Aquariid outbursts recorded in the classic Maya hieroglyphic script using orbital integrations". *Planetary and Space Sci.*, **144**, 112–125.

Miskotte K. (2019). "The Geminids of 2018: an analysis of visual observations". *eMeteorNews*, **4**, 207–212.

Rendtel J. (2004). "Evolution of the Geminids observed over 60 years". *Earth, Moon, and Planets*, **95**, 27–32.

Rendtel J. (2020). "Geminids 2018". In Pajer U., Rendtel J., and Verbeeck C., editors, *Proc. IMC Bollmannsruh, Germany, 2019*. IMO. In press.

Ryabova G. O. (2016). "A preliminary numerical model of the Geminid meteoroid stream". *MNRAS*, **456**, 78–84.

Ryabova G. O. and Rendtel J. (2018). "Increasing Geminid meteor shower actvity". *MNRAS*, **475**, L77–L80.

Handling Editor: David Asher
This paper has been typeset from a LaTeX file prepared by the author.

Identification of two new meteor showers: #797 EGR and #798 ACD

Lauriston de Sousa Trindade[1,2], *Marcelo Zurita*[2,3], *Alfredo Dal'ava Jr.*[2,4], *Gabriel Gonçalves Silva*[2,5], *and Carlos Augusto Bella Di Pietro*[2]

The Brazilian Meteor Observation Network – BRAMON – reports the discovery of two new meteor showers, initially observed after a search in its own database. For the meteor shower #797 EGR, it is listed one meteor in 2014, eight meteors in 2015 and three meteors in 2016 (two are in the BRAMON database and one in the EDMOND database), occurring between solar longitudes of 77° and 89°. The average radiant position is in right ascension of 342.3° and declination of −51.39°. For the meteor shower #798 ACD, it is listed two meteors in 2014 (one meteor in the BRAMON database and one meteor in the EDMOND database), eleven meteors in 2015 (ten meteors in the BRAMON database and one meteor in the base of EDMOND data), six meteors in 2016 and four meteors in 2017, occurring between solar longitudes of 120.7° and 139.7°. The average radiant position is in right ascension of 68.82° and declination of −38.15°.

Received 2019 July 2

1 Introduction

BRAMON is a meteor-monitoring network that was created in 2014 to record and study meteors over Brazil, which is in a privileged position in the southern hemisphere (Amaral et al., 2018b), as well as to provide more detailed information about high-luminosity bolides and other meteorites (Zurita et al., 2019). The result of this effort resulted in the production of a database made available together with the EDMOND database (Amaral et al., 2018a; EDMOND, 2018).

2 New showers

A video showing the evolution of the radiants of the meteors paired by BRAMON between the years 2014 and 2015 was created as a first analysis approach. It was observed, in both years, an unexpected concentration of meteors in the direction of the Grus constellation, always in mid-June. During the video analysis process, it was also noticed a meteor grouping that happened in the Caelum constellation repeating at the beginning of August. The calculations were performed following the methodology proposed by (Drummond, 1981), showing the existence of two small outbursts to be called epsilon Gruids (EGR) and August Caelids (ACD).

3 Methodology

As a first visual approach, it was adopted that a meteor cluster must have at least six members to be identified as a potential new shower (Jenniskens & Nenon, 2016). After the identification of those clusters, a stricter criterion was applied, identifying as new showers the clusters with more than ten members (Šegon et al., 2014) and whose orbits have the criterion of similarity of $D_D < 0.105$ in relation to the group average orbit. The similarity criterion was initially defined by (Southworth & Hawkins, 1963) in which the similarity between two orbits is defined as the distance between two points in a five-dimensional space, described by their conventional orbital parameters: q (perihelion distance), e (eccentricity), i (inclination), ω (perihelion argument) and Ω (longitude of the ascending node), as shown in Equation 1.

$$[D_{sh}]^2 = (e_2 - e_1)^2 + (q_2 - q_1)^2 + \left(2\sin\left(\frac{l_{21}}{2}\right)\right)^2 + \left(\frac{e_2 - e_1}{2}\right)^2 \left(2\sin\left(\frac{\Pi_{21}}{2}\right)\right) \quad (1)$$

where, suffix 1 and 2 refer to the two orbits to be compared, I_{21} is the angle between the planes of the two orbits, and Π_{21} is the angle between their respective perihelion points. These angles are defined in Equations 2 and 3, and Γ is defined in Equation 4.

$$I_{21} = \arccos[\cos(i_1)\cos(i_2) + \sin(i_1)\sin(i_2)\cos(\Omega_2 - \Omega_1)] \quad (2)$$

$$\Pi_{21} = \omega_2 - \omega_1 + 2\Gamma \arcsin\left(\cos\left(\frac{i_2 + i_1}{2}\right)\sin\left(\frac{\Omega_2 - \Omega_1}{2}\right)\sec\frac{i_{21}}{2}\right) \quad (3)$$

$$\Gamma = \begin{cases} +1, & |\Omega_2 - \Omega_1| \leq 180^\circ \\ -1, & |\Omega_2 - \Omega_1| > 180^\circ \end{cases} \quad (4)$$

Drummond (1981) proposed some modifications in the dissimilarity criterion of (Southworth & Hawkins, 1963), resulting in D-Drummond Criterion (D_D), whose definition is shown in Equation 5.

$$[D_D]^2 = \left(\frac{e_2 - e_1}{e_2 + e_1}\right)^2 + \left(\frac{q_2 - q_1}{q_2 + q_1}\right)^2 + \left(\frac{l_{21}}{180^\circ}\right)^2 + \left(\frac{e_2 + e_1}{2}\right)^2 \left(\frac{\theta_{21}}{180^\circ}\right)^2 \quad (5)$$

[1]Universidade Estadual do Ceará / UAB Pólo Maracanaú , Brazil. Email: lauristontrindade@yahoo.com.br
[2]Brazililian Meteor Observation Network - BRAMON, Nhandeara, Brazil. Email: bramon@bramonmeteor.org
[3]Associação Paraibana de Astronomia - APA, João Pessoa, Brazil. Email: marcelozurita@gmail.com
[4]Pontifícia Universidade Católica de Minas Gerais, Poços de Caldas, Brazil. Email: alfredojr@dalava.com.br
[5]Instituto de Química, Universidade de São Paulo, São Paulo, Brazil. Email: gabrielg@iq.usp.br

IMO bibcode WGN-476-trindade-identification
NASA-ADS bibcode 2019JIMO...47..184T

where, I_{21} is the angle between the two orbital planes defined in Equation 2, and θ_{21} is the angle between the perihelion points of each orbit, defined in Equation 6.

$$\theta_{21} = \arccos[\sin(\beta_1)\sin(\beta_2) + \cos(\beta_1)\cos(\beta_2)\cos(\lambda_2 - \lambda_1)] \quad (6)$$

where, λ and β are respectively the longitude and ecliptic latitude of the perihelion defined in Equations 7 and 8.

$$\lambda = \Omega + \arctan(\cos(i)\tan(\omega)) \quad (7)$$

$$\beta = \arcsin(\sin(i)\sin(\omega)) \quad (8)$$

Subsequently, other definitions were proposed by Jopek (1993) and by Valsecchi et al. (1999). However, for the validation of these showers it was used the criterion defined by Drummond (1981).

3.1 Identification of showers

The identification of the meteors was done using a visual approach. The epsilon Gruid meteors were initially identified in a visual analysis of an animation showing the radiant position of the recorded meteors identified during the first two years of BRAMON operation. The animation was composed of 731 frames, one for each night between 01/01/2014 and 12/31/2015. Each frame was generated using the UFOOrbit software (SonotaCo, 2009) and shows a celestial map with the radiant of all the meteors recorded in the previous 15 nights, in addition to the position of each meteor shower officially known that is active at the time. Observing the resulting animation, a concentration of supposedly "sporadic" meteors was observed between June 7 and 19, next to the Grus Constellation. Using the UFOOrbit software (SonotaCo, 2009), the orbital parameters of these meteors were extracted. They were numbered 19, with seven in the year 2014 and twelve in the year 2015. The August Caelids meteors were perceived during the use of the UFORadiant software (SonotaCo, 2009) while analyzing the BRAMON database in search of new meteors candidates for the epsilon Gruids shower. The orbital parameters of eight meteors were extracted, seven of them occurred in 2015 and one in 2016.

3.2 Dissimilarity test

At first, the average orbit of the meteors in initial cluster was obtained. Then, the dissimilarity between this average orbit and each meteor in the cluster was calculated using the D Criterium (Drummond, 1981). All meteors of the cluster with D Criterium smaller than 0.105 were maintained while the others were discarded. A new average orbit was calculated for the remaining meteors and dissimilarity was calculated again for each member of the new cluster. The process was repeated until the number of members of the cluster stabilized. As a minimum limit of six meteors in two distinct years to was achieved, the cluster can be reported as a potential annual meteor shower. Lastly, the dissimilarity test was used in a search for a parental body of the proposed showers. The dissimilarity between the average orbit of these showers and the objects of the Comet and near-Earth asteroid databases was calculated as done by (Šegon et al., 2013).

3.3 Nomenclature

Based on a proposal from (Jenniskens, 2008), a meteor shower name is defined by the constellation that has the star closest to its radiant, using the possessive form of Latin followed by the suffix id or ids. If greater precision is required, the name should include the Greek letter from the name of the brightest star closest to the radiant. One can opt to add the name of the month of the shower peak to its name to distinguish it from other showers in the same constellation. Following these criteria, the names defined for the showers were epsilon Gruids, for its radiant being next to the star epsilon Gruis, and August Caelids, for their radiant being in the Caelum constellation and its maximum occurring in the month of August. The acronyms must be unique, containing three letters and approaching the spelling of the name of the shower. For epsilon Gruids, the acronym EGR was defined and the 797 number was designated by the Meteor Data Center. For the August Caelids, ACD along with the 798 number.

4 Results

4.1 EGR – epsilon Gruids

After the initial report to the IAU, new meteors linked to the shower were registered by BRAMON, maintaining the orbital dissimilarity criterion. The records were distributed as follows: 2014 – one meteor; 2015 – eight meteors; 2016 – three meteors. The meteors of the Grus constellation cluster occurred from June 7 to 19 with an average solar longitude of 81.°37 (J2000.0). The mean radiant position of shower # 797 EGR was determined to be under the point with R.A. = 342.°28 and Dec = −51.°39. The average geocentric velocity of the meteors is 52.86 km/s, the mean daily motion of the radian was estimated as ΔR.A. = 1.°1/day and ΔDec = 0.°0/day. No parental body candidates

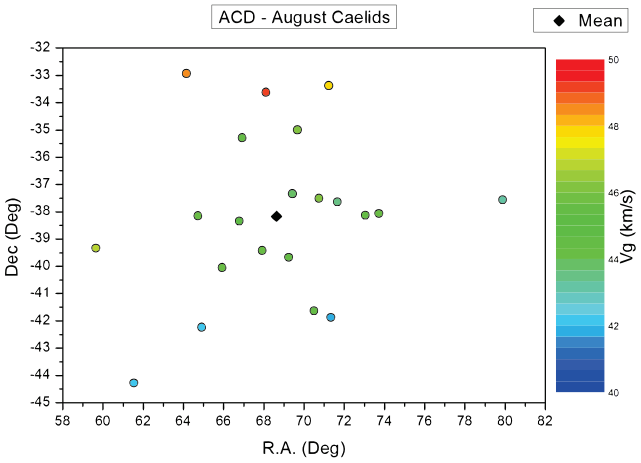

Figure 1 – Distribution of meteors (with geocentric velocities) around the mean position of the epsilon Gruids radiant.

Table 1 – List of the Meteors (#797 EGR). Meteors labelled with a * are from the EDMOND database.

Meteor	$\lambda_\odot$	R.A	Dec	Vg	a	e	q	Peri	Node	i	D_D
20140613-081309	82.06	341.08	−53.24	52.20	9.40	0.92	0.72	66.62	262.06	95.90	0.037
20150607-064431	76.02	339.52	−50.90	53.10	3.62	0.79	0.75	65.60	256.00	103.10	0.069
20150609-051055	77.87	340.01	−52.41	53.74	7.99	0.91	0.76	62.40	257.90	100.60	0.041
20150610-020603	78.70	333.89	−52.32	53.70	15.90	0.96	0.67	71.76	258.70	99.35	0.070
20150612-034607	80.68	342.34	−53.76	50.90	4.51	0.84	0.74	66.20	260.70	95.00	0.038
20150613-023001	81.59	348.81	−50.42	51.60	3.39	0.77	0.78	62.80	261.60	98.90	0.075
20150614-051655	82.65	343.37	−52.42	51.80	5.67	0.87	0.73	66.61	262.60	96.44	0.025
20150614-054050	82.34	343.95	−52.77	52.80	11.36	0.93	0.75	62.40	263.58	97.00	0.044
20150615-044227	83.58	339.94	−50.83	53.11	10.21	0.93	0.68	71.84	261.39	98.54	0.056
20160612-035508	81.40	339.81	−51.95	51.65	4.94	0.86	0.71	69.98	261.39	96.78	0.032
20160613-054413*	—	—	—	51.20	4.75	0.85	0.70	70.80	261.5	105.00	0.051
20160619-081923	88.26	352.39	−44.27	55.62	6.36	0.88	0.76	61.86	268.53	107.48	0.073
Mean	81.37	342.28	−51.39	52.86	7.36	0.88	0.73	66.60	261.43	99.50	0.05

were found using the dissimilarity test between the average orbit of the shower # 797 EGR and the objects in the Comet and near-Earth asteroid databases. Details of the shower orbital parameters can be seen in Table 1 and the distribution of the meteors around the radiant is shown in Figure 1.

4.2 ACD – August Caelids

Again, after the initial report to the IAU, new meteors registered by BRAMON were added to the shower, maintaining the criterion of orbital dissimilarity. The records were distributed as follows: 2014 – one meteor; 2015 – eleven meteors; 2016 – six meteors; 2017 – four meteors. The meteors of the Caelum constellation cluster occurred from July 23 to August 12, with average solar longitude of 131.°38 (J2000.0). The average radiant position of shower # 798 ACD was determined to be under the point with R.A. = 68.°82 and Dec = −38.°15. The average geocentric velocity of the meteors is 44.87 km/s, the mean daily motion of the radian was estimated as ΔR.A. = 0.°54/day and ΔDec = 0.°13/day. Again, no parental body candidates were found using the dissimilarity test between the average orbit of the shower # 798 ACD and the objects in the Comet and near-Earth asteroid databases. Details of the orbital parameters can be seen in Table 2 and the distribution of the meteors around the radiant is shown in Figure 2.

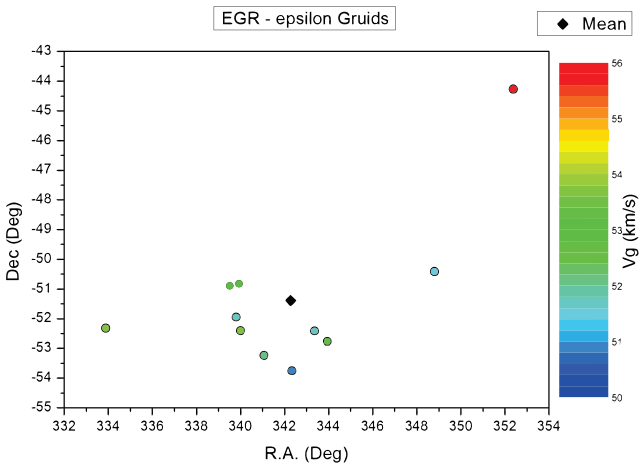

Figure 2 – Distribution of meteors (with geocentric velocities) around the mean position of the August Caelids radiant.

5 Conclusion

The discovery of two meteor showers in such a short time of operation of such a new meteor monitoring network demonstrates the potential of showers yet to be unveiled on the southern hemisphere. This potential can be exploited by BRAMON due to the privileged position of its stations distributed throughout Brazil and to the large number of operators integrating the network. In addition, the association of BRAMON with other initiatives such as the SONEAR Observatory can help on the search for parental bodies associated with the newly confirmed showers and future finds.

Acknowledgements

The authors want to thank all the operators that participate in the BRAMON and especially thank to Cristóvão Jacques, Carlos Jung and Jakub Koukal, who guided us through the calculations and other struggles concerning the discoveries. The authors also want to thank the colleagues in the science media and science popularizers that covered the first announcements of the identification of the new showers. Lastly, the authors want to thank professor Fabio Rodrigues and Dr. Douglas Galante that helped in the writing and grammatical reviews of this work.

References

Amaral L. S., Bella C. A. P. B., Trindade L. S., Zurita M. L. P. V., Silva G. G., Domingues M. W. S., Poltronieri R. C., Faria C. J. L., and Jung C. F. (2018a). "A search method for meteor radiants". *WGN, Journal of the IMO*, **46**, 191–197.

Amaral L. S., Trindade L. S., Bella C. A. P. B., Zurita M. L. P. V., Poltronieri R. C., Silva G. G., Faria C. J. L., Jung C. F., and Koukal J. A. (2018b). "Brazilian Meteor Observation Network: History

Table 2 – List of the Meteors (#798 ACD). Meteors labelled with a * are from the EDMOND database.

Meteor	$\lambda_\odot$	R.A	Dec	Vg	a	e	q	Peri	Node	i	D_D
20140801-082848*	—	—	—	44.44	4.65	0.78	1.000	347.6	308.8	78.87	0.037
20140804-072928	131.67	70.74	−37.51	46.26	13.66	0.928	0.982	339.0	311.7	80.07	0.068
20150803-080134	130.47	66.78	−38.34	45.10	4.61	0.780	0.100	343.6	310.5	80.30	0.024
20150803-082609	130.49	66.92	−35.29	45.47	3.46	0.715	0.984	338.1	310.5	82.62	0.068
20150803-082609*	—	—	—	46.20	4.16	0.760	0.980	338.4	310.5	83.40	0.043
20150804-080655	131.43	67.92	−39.42	44.30	4.73	0.790	1.000	344.5	311.4	78.50	0.021
20150805-060514	132.31	71.66	−37.64	43.59	4.37	0.778	0.972	334.8	312.3	76.97	0.039
20150807-081437	134.31	73.72	−38.07	44.30	5.83	0.830	0.980	337.3	314.3	77.50	0.030
20150808-064000	135.21	69.67	−35.00	46.30	4.15	0.760	0.990	339.8	315.2	83.40	0.051
20150808-074553	135.25	71.33	−41.88	41.80	4.02	0.750	1.000	346.6	315.3	73.50	0.063
20150808-084713	135.29	69.42	−37.34	43.68	3.18	0.686	0.997	343.4	315.3	78.99	0.089
20150811-055544	138.05	70.49	−41.63	44.50	14.19	0.929	1.007	350.3	318.1	76.23	0.098
20150723-083249	120.69	59.64	−39.34	46.75	7.86	0.873	1.000	345.0	300.7	82.48	0.082
20160725-043910	122.44	61.53	−44.28	42.18	4.74	0.788	1.005	347.6	302.4	73.85	0.075
20160726-081137	123.54	64.15	−32.93	48.40	5.94	0.839	0.956	330.6	303.5	87.05	0.085
20160805-062223	133.03	68.11	−33.62	49.02	10.9	0.910	0.981	338.7	313.1	86.82	0.075
20160805-074642	133.09	73.04	−38.13	45.44	13.7	0.928	0.980	338.3	313.1	78.18	0.070
20160806-081216	134.06	69.24	−39.67	44.59	6.38	0.843	1.002	346.9	314.1	78.01	0.040
20160812-055149	139.72	71.23	−33.38	47.94	6.11	0.838	0.990	341.6	319.7	85.70	0.076
20170724-061921	121.31	65.92	−40.05	44.08	6.77	0.856	0.975	335.9	301.3	76.48	0.085
20170730-071856	127.09	64.91	−42.24	42.06	3.79	0.735	1.004	347.0	307.1	74.50	0.068
20170806-073702	133.80	64.72	−38.15	44.30	3.21	0.686	1.009	350.6	313.8	80.44	0.096
20170807-060147	134.69	79.88	−37.56	43.18	9.13	0.897	0.939	327.6	314.7	73.46	0.092
Mean	131.33	68.62	−38.17	44.94	6.5	0.81	0.99	341.4	311.1	79.45	0.065

of creation and first developments". In Gyssens M. and Rault J.-L., editors, *Proceedings of the International Meteor Conference, Petnica, Serbia 21-24 September, 2017*. IMO, pages 171–175.

Drummond J. D. (1981). "A test of comet and meteor shower associations". *Icarus*, **45**, 545–553.

EDMOND (2018). "EDMOND Database". `http://www.daa.fmph.uniba.sk/edmond` .

Jenniskens P. (2008). "The IAU meteor shower nomenclature rules". *Earth, Moon and Planets*, **102**, 5–9.

Jenniskens P. and Nenon Q. (2016). "CAMS verification of single-linked high-threshold D-criterion detected meteor showers". *Icarus*, **266**, 371–383.

Jopek T. J. (1993). "Remarks on the meteor orbit similarity D-criterion". *Icarus*, **106**, 603–607.

Šegon D., Andreić Ž., Korlević K., Novoselnik F., Vida D., and Skokić I. (2013). "8 new showers from Croatian Meteor Network data". *WGN, Journal of the IMO*, **41**, 70–74.

Šegon D., Gural P., Andreić Ž., Skokić I., Korlević K., Vida D., and Novoselnik F. (2014). "A parent body search across several video meteor data bases". In Jopek T. J., Rietmeijer F. J. M., Watanabe J., and Williams I. P., editors, *The Meteoroids 2013, Proceedings of the Astronomical Conference held at A.M. University, Poznań, Poland, Aug. 26-30, 2013*. A.M. University Press, pages 251–262.

SonotaCo (2009). "A meteor shower catalog based on video observations in 2007-2008". *WGN, Journal of the IMO*, **37**, 55–62.

Southworth R. B. and Hawkins G. S. (1963). "Statistics of meteor streams". *Smithsonian Contributions to Astrophysics*, **7**, 261.

Valsecchi G. B., Jopek T. J., and Froeschlé C. (1999). "Meteoroid stream identification: a new approach - I. Theory". *Mon. Not. R. Astron. Soc.*, **304**, 743–750.

Zurita M., Damigle R., Di Pietro C., Trindade L., Silva G. G., Lima A., Mota A., Arthur R., and Betzler A. S. (2019). "A bright fireball over the coast of the state of Bahia". *Boletim da Sociedade Astronômica Brasileira*, **31**, 14–16.

Handling Editor: Željko Andreić

Preliminary results

Results of the IMO Video Meteor Network — October 2018

Sirko Molau[1], *Stefano Crivello, Rui Goncalves, Carlos Saraiva, Enrico Stomeo, Jörg Strunk, Javor Kac*

During 2018 October, 82 cameras of the IMO Video Meteor Network recorded almost 75 000 meteors during more than 13 700 hours of observing time. The flux density profile of the October Camelopardalids is presented. It shows a maximum of 7 meteoroids per 1 000 km^2 per hour at $\lambda_\odot = 192^\circ.47$, with the FWHM being of only $0^\circ.07$ solar longitude. The Draconids presented a strong outburst on 2018 October 8/9, confirming predictions. The flux density profile shows complex structure with at least three significant peaks. The highest peaks were observed at 22^h50^m UT ($195^\circ.35$ solar longitude) and at 23^h50^m UT ($135^\circ.39$ solar longitude) with a flux density of 90 meteoroids per 1 000 km^2 per hour. Flux density profiles are also presented for the October Ursae Majorids and the Orionids with both showers showing similar activity profiles in 2018 when compared with their average profiles from previous years.

Received 2019 December 23

1 Introduction

The perfect observing conditions of the previous months continued until mid-October. 78 out of 82 video cameras were in operation on October 4/5, and overall 65 cameras managed to observe during twenty or more observing nights. It was only in the final ten days that the observing conditions deteriorated significantly and at some observing sites breaks of more than a week resulted from poor weather. In total we collected over 13 700 hours of effective observing time (Table 1 and Figure 1), making it the best October result ever and the fourth best output of any month in the history of the IMO Network. In addition, the meteor total of almost 75 000 marked a record for this month, which is in part thanks to the Draconids which we will discuss later. First, we want to welcome Stefano Missiaggia, who has been supporting our network since October 2018. He operates a Mintron camera named Toaldo with a 4.5 mm $f/1.2$ lens from the small city of Nove in northern Italy.

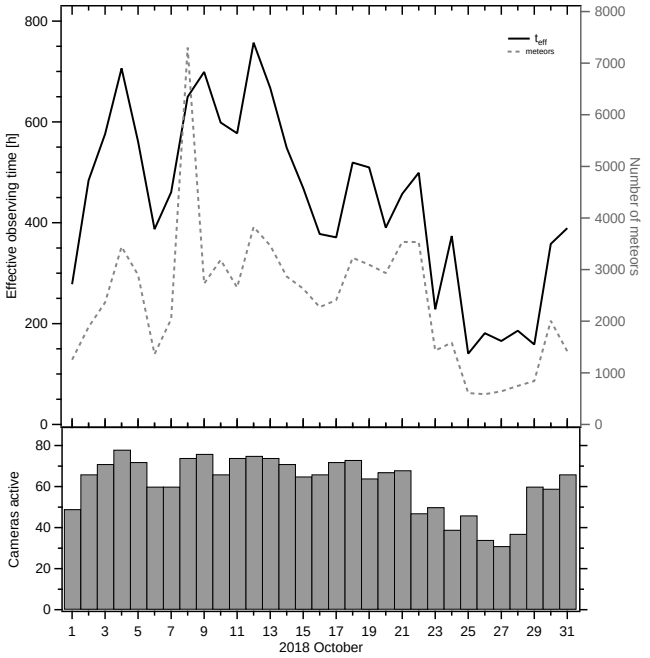

Figure 1 – Monthly summary for the effective observing time (solid black line), number of meteors (dashed gray line) and number of cameras active (bars) in 2018 October.

2 October Camelopardalids

In time order, the October Camelopardalids were the first relevant shower of October. It has a small full-width-at-half-maximum (FWHM) and can only be recorded by the IMO network if the peak falls within the European nighttime hours. From the years 2011–2016 we had recently derived a peak time of $192^\circ.59$ solar longitude with an activity of about 7 meteoroids per 1 000 km^2 per hour. In 2017 the peak was somewhat early ($192^\circ.50$ solar longitude). It was also stronger than in earlier years with a flux density exceeding 25 meteoroids per 1 000 km^2 per hour (Molau et al., 2018). Hence, for 2018 we expected the peak on October 6 between 02^h and 04^h UT. The small waxing crescent moon hardly disturbed the observations, and the weather was also favorable for observers in central Europe – perfect conditions to analyze this shower in more detail.

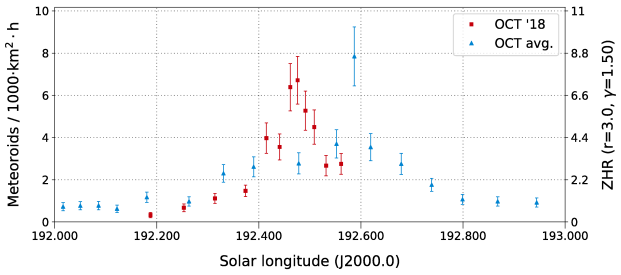

Figure 2 – Comparison of the flux density profile of the October Camelopardalids 2018 (darker/red) and in the average of 2011–2016 (lighter/blue), derived from video data of the IMO Network.

[1]Abenstalstr. 13b, 84072 Seysdorf, Germany.
Email: sirko@molau.de

IMO bibcode WGN-476-molau-vidoct
NASA-ADS bibcode 2019JIMO...47..188M

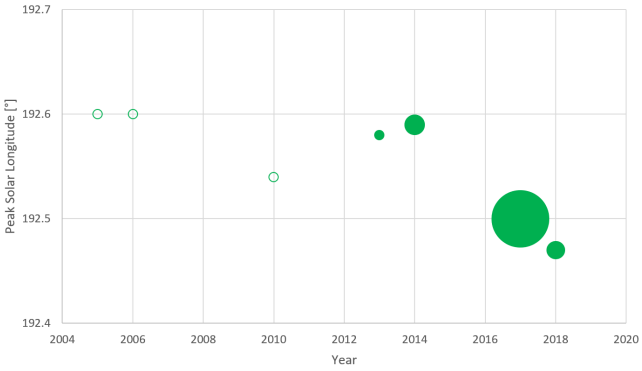

Figure 3 – Time (Y axis) and strength (diameter) of maximum of the October Camelopardalids in the years 2005 to 2018. If no data point is given, the peak was outside the European nighttime hours or the data set was too small. Open circles represent years without flux density measure from which we only know the time of maximum.

Indeed, the cameras of the IMO Network managed to record almost 350 October Camelopardalids during the night of October 5/6 – more than in the earlier years. Figure 2 shows a "perfect" activity profile with highest rates near 01^{h} UT (192.°47 solar longitude), i.e. three hours earlier than in the long-term average. The flux density was up to 7 meteoroids per 1 000 km^2 per hour and in line with the long-term average. The FWHM was only 0.°07 solar longitude, corresponding to about two hours. Thus, the peak was shorter than in previous years, but longer than in 2017. With $r = 1.95$, the population index of the Camelopardalids was much smaller than the sporadic population index ($r = 2.7$), i.e. the shower comprised of many bright meteors.

Since the peak time seems to vary, we had a closer look at the maxima since the discovery of the shower back in 2005. Figure 3 depicts the time of peak vs. year. The size of the bullets represents the strength of the peak. Note that we have no flux density data before 2011, so until 2010 we can only estimate the peak time (based on the absolute number of shower meteors uncorrected for the limiting magnitude and effective observing time), but not the strength. We can see that in all the years between 2005 and 2014 the peak occurred at about 192.°60 solar longitude. Only in 2017 and 2018 was it early. In the future we will see if this trend continues and reflects the evolution of the meteor shower.

3 Draconids

Only three nights later we could observe the Draconids in central Europe, on which we have already reported elsewhere (e.g. in German VdS-Journal No. 71). Forecasts by different authors (Mikiya Sato, Jeremie Vaubaillon, Mikhail Maslov) had predicted enhanced activity of up to ZHR 50 on October 8/9 close to midnight, caused by a dust trail from 1953 (Rendtel, 2017; Maslov, 2011). Indeed, a strong outburst was detected visually (International Meteor Organization, 2018) and with our video equipment. During this night we recorded over 4 000 shower members. Thanks to the large quantity, we could derive a high-resolution activity profile showing a complex structure (Figure 4).

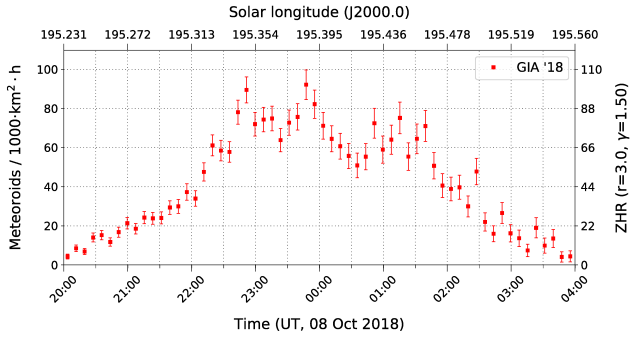

Figure 4 – High resolution flux density profile of the Draconids on 2018 October 8/9, derived from video data of the IMO Network

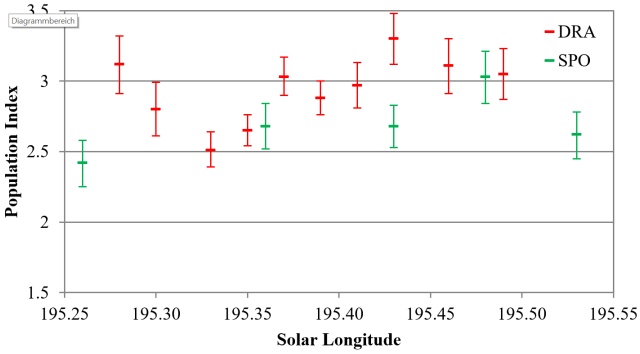

Figure 5 – Population index of the Draconids (darker/red) and the sporadic meteors (lighter/green) on 2018 October 8/9.

The first peak was observed at $22^{h}50^{m}$ UT (195.°35 solar longitude) with a flux density of 90 meteoroids per 1 000 km^2 per hour, calculated with a population index of $r = 3.0$. Another peak of the same strength occurred one hour later at $23^{h}50^{m}$ UT (135.°39 solar longitude). Thereafter the rate seemed to decline, but the trend reversed at $00^{h}35^{m}$ UT. Around $01^{h}15^{m}$ UT (135.°45 solar longitude) a tertiary peak was observed. Rates were highly variable at that time, so depending on the chosen resolution even two tertiary peaks can be recognized.

The maximum ZHR of the Draconids as obtained from video was about 100, i.e. several times the predicted value. The population index (Figure 5) scattered around $r = 3.0$ and was larger than the sporadic population index ($r = 2.7$).

Visual observations of IMO (International Meteor Organization, 2018) revealed a peak ZHR of 160 at $22^{h}45^{m}$ UT (using $r = 3.0$) and another outlier close to midnight, which matches well with our video data. The tertiary peak is not visible in the visual data.

Figure 6 gives an impression from the outburst by combining the recordings of the cameras Remo1 to Remo4 in Ketzür, Germany into a single panoramic image. The impression that there were fewer Draconids at the center of the image is an illusion. The region involved corresponds to overlapping fields of view belonging to one camera that recorded in the evening hours and another one that recorded in the morning hours when there were fewer shower meteors than at midnight.

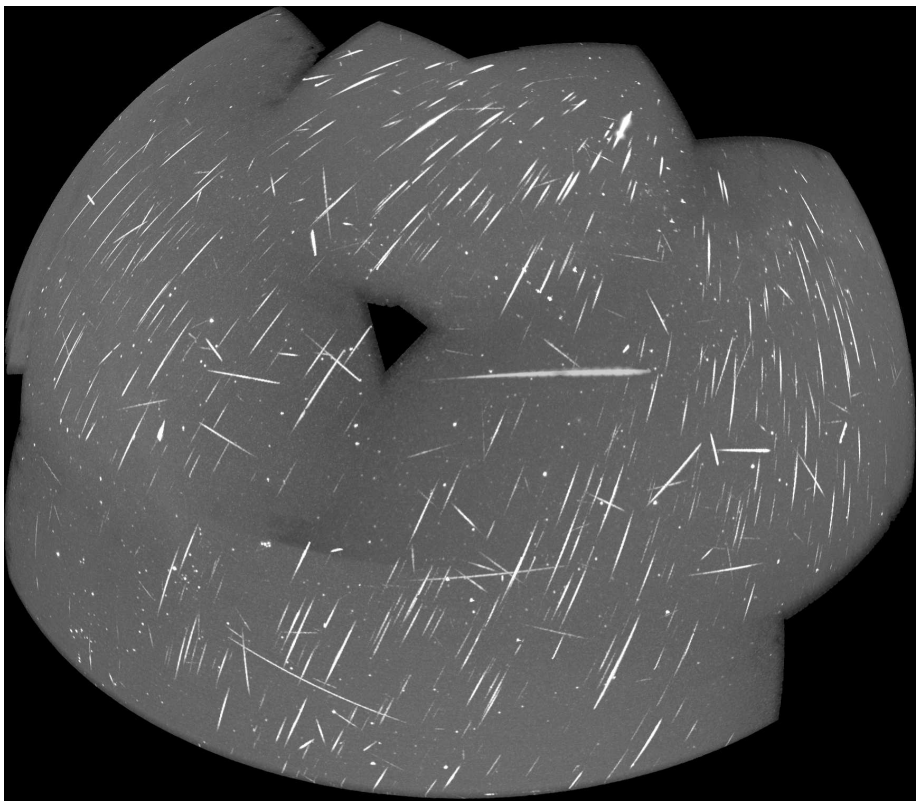

Figure 6 – Panoramic image of the Draconids from recordings of Remo1 to Remo4 in Ketzür on 2018 October 8/9.

4 October Ursae Majorids

The other meteor showers of October are briefly summarized. The 2018 activity profile of the October Ursae Majorids fits well with the long-term average for the years 2011 to 2017 (Figure 7), although the sharp peak at 202°.1 solar longitude was not observed this year. The peak flux density was again about 4 meteoroids per 1 000 km^2 per hour and with $r = 2.6$ the population index was 0.2 smaller than the sporadic r-value.

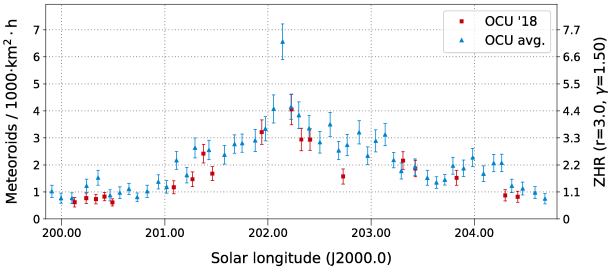

Figure 7 – Comparison of the flux density profile of the October Ursae Majorids in 2018 (darker/red) and in the average of 2011–2017 (lighter/blue), derived from video data of the IMO Network.

5 Orionids

The activity profile of the Orionids was also in line with the long-term average with respect to shape and strength. The peak was just a little delayed. The large scatter in the descending activity branch results from the poor weather conditions and the corresponding smaller number of meteors. The population index of the Orionids in 2018 was only a little smaller than the r-value of the sporadic meteors.

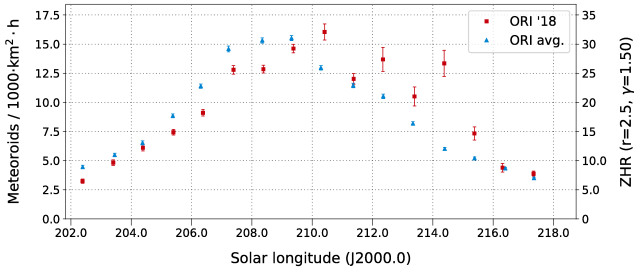

Figure 8 – Comparison of the flux density profile of the Orionids in 2018 (darker/red) and in the average of 2012–2017 (lighter/blue), derived from video data of the IMO Network.

References

International Meteor Organization (2018). "Draconids 2018 campaign Live Graph". `http://www.imo.net/members/imo_live_shower/summary?shower=DRA&year=2018` .

Maslov M. (2011). "Future Draconid outbursts (2011 – 2100)". *WGN, Journal of the IMO*, **39:3**, 64–67.

Molau S., Crivello S., Goncalves R., Saraiva C., Stomeo E., Strunk J., and Kac J. (2018). "Results of the IMO Video Meteor Network – October 2017". *WGN, Journal of the IMO*, **46:4**, 136–141.

Rendtel J. (2017). "2018 Meteor Shower Calendar". International Meteor Organization. IMO_INFO(2-17).

Handling Editor: Javor Kac

Code	Name	Location	Camera	FOV [°²]	Stellar LM [mag]	Eff.CA [km²]	Nights	Time [h]	Meteors
ARLRA	Arlt	Ludwigsfelde/DE	Ludwig2 (0.8/8)	1483	6.2	3812	29	194.7	1751
BERER	Berkó	Ludányhalászi/HU	Hulud1 (0.8/3.8)	5524	4.8	3829	19	167.8	1021
BIATO	Bianchi	Mt. San Lorenzo/IT	Omsl1 (1.2/4)	6422	4.0	1699	24	144.3	658
BOMMA	Bombardini	Faenza/IT	Mario (1.2/4.0)	5779	3.3	644	28	202.2	1053
BREMA	Breukers	Hengelo/NL	Mbb3 (0.75/6)	2399	4.2	641	23	169.6	461
BRIBE	Klemt	Herne/DE	Hermine (0.8/6)	2369	4.2	674	26	201.4	1112
		Bergisch Gladbach/DE	Klemoi (0.8/6)	2374	4.6	1123	26	213.5	1137
CARMA	Carli	Monte Baldo/IT	Bmh2 (1.5/4.5)*	4243	3.0	371	28	166.1	1743
CASFL	Castellani	Monte Baldo/IT	Bmh1 (0.8/6)	2402	5.0	1633	28	194.4	839
CINFR	Cineglosso	Faenza/IT	Jenni (1.2/4)	5995	3.9	1240	29	214.3	1033
CRIST	Crivello	Valbrevenna/IT	Arci (0.8/3.8)	5566	4.6	2571	22	156.1	1030
			Bilbo (0.8/3.8)	5441	4.2	1764	22	177.2	1409
			C3P8 (0.8/3.8)	5489	4.2	1603	22	165.9	902
			Stg38 (0.8/3.8)	5574	4.4	1905	22	101.7	1247
ELTMA	Eltri	Venezia/IT	Met38 (0.8/3.8)	5607	4.3	2381	26	181.4	986
FORKE	Förster	Carlsfeld/DE	Akm3 (0.75/6)	2387	5.1	2145	18	151.8	1041
GONRU	Goncalves	Foz do Arelho/PT	Farelho1 (0.75/4.5)	2260	3.0	206	16	99.2	119
		Tomar/PT	Templar1 (0.8/6)	2212	5.3	1873	27	236.7	1418
			Templar2 (0.8/6)	2341	5.0	1718	27	235.3	1184
			Templar3 (0.8/8)	1438	4.3	542	25	192.2	493
			Templar4 (0.8/3.8)	5180	3.0	497	27	233.9	1076
			Templar5 (0.75/6)	2309	5.0	2248	25	185.0	968
GOVMI	Govedič	Središče ob Dravi/SI	Orion2 (0.8/8)	1471	5.5	2170	28	128.1	476
			Orion3 (0.95/5)	3152	4.9	2130	25	153.6	247
			Orion4 (0.95/5)	3818	4.3	1634	25	150.4	223
HERCA	Hergenrother	Tucson/US	Salsa3 (0.8/3.8)	2336	4.1	538	20	175.6	627
HINWO	Hinz	Schwarzenberg/DE	Hinwo1 (0.75/6)	2375	5.1	1889	20	179.1	1068
IGAAN	Igaz	Budapest/HU	Hupol (1.2/4)	2414	3.6	409	26	160.7	160
JONKA	Jonas	Budapest/HU	Husor (0.95/4)	3988	3.6	729	25	188.7	382
			Husor2 (0.95/3.5)	2468	3.9	716	25	194.0	397
KACJA	Kac	Kamnik/SI	Cvetka (0.8/3.8)*	5334	4.3	2028	10	71.3	399
			Rezika (0.8/6)	2269	4.4	863	14	95.8	761
			Stefka (0.8/3.8)	5458	3.6	911	10	74.3	264
		Ljubljana/SI	Sraka (0.8/6)	2348	4.8	1595	21	113.5	465
KOSDE	Koschny	La Palma/ES	Icc9 (0.85/25)*	660	6.7	2835	28	185.1	2436
			Lic2 (3.2/50)*	1933	6.5	6554	28	132.8	1625
LOJTO	Łojek	Grabniak/PL	Pav57 (1.0/5)	728	6.2	2087	5	45.4	347
MACMA	Maciejewski	Chełm/PL	Pav35 (0.8/3.8)	5329	4.0	1530	25	163.2	708
			Pav36 (0.8/3.8)*	5484	4.0	1501	25	200.1	1051
			Pav43 (0.75/4.5)*	2251	4.7	1484	20	147.3	781
			Pav60 (0.75/4.5)	2302	5.1	1803	19	153.9	1160

Table 1 – Observers contributing to 2018 October data of the IMO Video Meteor Network. Eff.CA designates the effective collection area; the overall number of nights is the number of nights with at least one camera operating, the overall observing time and number of meteors are sums over all cameras.

Table 1 – Observers contributing to 2018 October data of the IMO Video Meteor Network – continued from previous page.

Code	Name	Location	Camera	FOV [°²]	Stellar LM [mag]	Eff.CA [km²]	Nights	Time [h]	Meteors
MARRU	Marques	Lisbon/PT	Ran1 (1.4/4.5)	4395	4.0	1330	28	214.4	1050
MASMI	Maslov	Novosibirsk/RU	Nowatec (0.8/3.8)	5559	3.6	827	11	63.1	439
MISST	Missiaggia	Nove/IT	Toaldo (1.2/4.5)	4329	4.6	2049	24	172.5	1511
MOLSI	Molau	Seysdorf/DE	Avis2 (1.4/50)*	1204	6.9	5982	26	194.5	2463
			Dimcam1 (0.8/8)	1553	6.8	10447	24	170.5	2467
			Escimo2 (0.85/25)	154	8.1	3828	25	199.7	574
		Ketzür/DE	Remo1 (0.8/8)	1467	6.5	5459	19	156.4	1751
			Remo2 (0.8/8)	1479	6.4	5037	19	168.1	1833
			Remo3 (0.8/8)	1422	6.4	4207	19	179.6	1495
			Remo4 (0.8/8)	1478	6.5	5355	19	178.1	2106
MORJO	Morvai	Fülöpszállás/HU	Huful (1.4/5)	3666	3.8	805	27	197.4	359
MOSFA	Moschini	Rovereto/IT	Rover (1.4/4.5)	3868	4.2	1240	25	162.7	583
NAGHE	Nagy	Budapest/HU	Hukon (0.8/3.8)	5475	4.0	1583	30	193.2	899
		Zamardi/HU	Huzam (0.8/6)	2359	4.7	1340	8	65.1	154
OCHPA	Ochner	Albiano/IT	Albiano (1.2/4.5)	3013	4.3	886	20	157.9	490
OTTMI	Otte	Pearl City/US	Orie1 (1.4/5.7)	2317	3.8	373	15	61.5	160
PERZS	Perkó	Becsehely/HU	Hubec (0.8/3.8)*	5557	2.9	470	23	149.7	562
ROTEC	Rothenberg	Berlin/DE	Armefa (0.8/6)	2359	4.5	907	24	198.6	688
SARAN	Saraiva	Carnaxide/PT	Ro1 (0.75/6)	2354	4.0	536	24	176.3	435
			Ro2 (0.75/6)	2365	4.1	635	28	220.3	738
			Ro3 (0.8/12)	720	5.7	1126	28	215.9	931
			Ro4 (1.0/8)	1568	4.2	546	28	216.4	296
			Sofia (0.8/12)	726	4.8	516	30	222.6	578
SCALE	Scarpa	Alberoni/IT	Leo (1.2/4.5)*	4170	4.5	2044	29	180.3	349
SCHHA	Schremmer	Niederkrüchten/DE	Doraemon (0.8/3.8)	5522	4.7	3184	26	158.2	625
SLAST	Slavec	Ljubljana/SI	Kayak1 (1.8/28)	1074	5.7	2642	18	87.2	162
			Kayak2 (0.8/12)	742	5.7	1052	18	116.3	154
STOEN	Stomeo	Scorze/IT	Min38 (0.8/3.8)	5587	4.5	2362	28	196.7	1834
			Noa38 (0.8/3.8)	5612	4.2	1889	26	203.3	1607
			Sco38 (0.8/3.8)	5583	4.8	3304	26	194.3	1822
STRJO	Strunk	Herford/DE	Mincam2 (0.8/6)	2355	5.6	3423	26	209.2	1934
			Mincam3 (0.8/6)	2302	4.5	1150	26	202.2	917
			Mincam4 (0.8/6)	2274	4.7	1001	26	202.7	587
			Mincam5 (0.8/6)	1481	6.0	3200	26	208.3	1169
			Mincam6 (0.8/6)	2396	5.3	2748	26	202.7	1018
TEPIS	Tepliczky	Agostyán/HU	Huago (0.75/4.5)	2428	4.6	1247	25	175.9	638
			Humob (0.8/6)	2388	4.6	1225	21	157.4	552
WEGWA	Wegrzyk	Nieznaszyn/PL	Pav78 (0.8/6)	2376	4.4	1264	21	138.6	483
YRJIL	Yrjölä	Kuusankoski/FI	Finexcam (0.8/6)	2315	5.5	2769	20	151.8	670
ZAKJU	Zakrajšek	Petkovec/SI	Petka (0.8/8)	1431	5.6	1956	25	155.8	1060
			Tacka (0.8/12)	715	5.3	784	24	152.6	386
* active field of view smaller than video frame						Overall	31	13 725.6	74 787

The International Meteor Organization

www.imo.net

Follow us on Facebook InternationalMeteorOrganization

Follow us on Twitter @IMOMeteors

Council

President: Cis Verbeeck,
Bogaertsheide 5, 2560 Kessel, Belgium.
e-mail: cis.verbeeck@scarlet.be

Vice-President: Juraj Tóth,
Fac. Math., Phys. & Inf., Comenius Univ.,
Mlynska dolina, 84248 Bratislava, Slovakia.
e-mail: toth@fmph.uniba.sk

Secretary-General: Robert Lunsford,
14884 Quail Valley Way, El Cajon,
CA 92021-2227, USA. tel. +1 619 755 7791
e-mail: lunro.imo.usa@cox.net

Treasurer: Marc Gyssens, Heerbaan 74,
B-2530 Boechout, Belgium.
e-mail: marc.gyssens@uhasselt.be
BIC: GEBABEBB
IBAN: BE30 0014 7327 5911
Bank transfer costs are always at your expense.

Other Council members:

Megan Argo, Jodrell Bank Centre for Astrophysics,
Alan Turing building, University of Manchester,
Oxford Road, Manchester, M13 9PL, UK.
e-mail: megan.argo@gmail.com

Javor Kac (see details under WGN)

Detlef Koschny, Zeestraat 46,
NL-2211 XH Noordwijkerhout, Netherlands.
e-mail: detlef.koschny@esa.int

Masahiro Koseki, 4-3-5 Annaka, Annaka-shi,
Gunma-ken 379-0116, Japan.
e-mail: geh04301@nifty.ne.jp

Sirko Molau, Abenstalstraße 13b, D-84072 Seysdorf,
Germany. e-mail: sirko@molau.de

Jean-Louis Rault, Société Astronomique de France,
16, rue de la Vallée, 91360 Epinay sur Orge,
France. e-mail: f6agr@orange.fr

Jürgen Rendtel, Eschenweg 16, D-14476 Marquardt,
Germany. e-mail: jrendtel@aip.de

Galina Ryabova, Res. Inst. of Appl. Math. & Mech.,
Tomsk State University, Lenin pr. 36, build. 27,
634050 Tomsk, Russian Federation.
e-mail: ryabova@niipmm.tsu.ru

Damir Šegon, J. Rakovca 3, 52100 Pula, Croatia.
e-mail: damir.segon@pu.t-com.hr

Commission Directors

Visual Commission: Rainer Arlt (rarlt@aip.de)
Generic e-mail address: visual@imo.net
Electronic visual report form:
http://www.imo.net/visual/report/electronic

Video Commission: Sirko Molau (video@imo.net)

Photographic Commission: Bill Ward
(William.Ward@glasgow.ac.uk)
Generic e-mail address: photo@imo.net

Radio Commission: Jean-Louis Rault (radio@imo.net)

Fireballs: Online fireball reports:
http://fireballs.imo.net

Outreach Officer

Jure Atanackov, e-mail: jureatanackov@gmail.com

Webmaster

Karl Antier, e-mail: webmaster@imo.net

WGN

Editor-in-chief: Javor Kac
Na Ajdov hrib 24, SI-2310 Slovenska Bistrica,
Slovenia. e-mail: wgn@imo.net;
include METEOR in the e-mail subject line

Editorial board: Ž. Andreić, M. Argo, D.J. Asher,
F. Bettonvil, J. Correira, M. Gyssens,
C. Hergenrother, T. Heywood, J.-L. Rault,
J. Rendtel, C. Verbeeck, S. de Vet, D. Vida.

IMO Sales

Available from the Treasurer or the Electronic Shop on the IMO Website	€	$
IMO membership, including subscription to WGN Vol. 47 (2019)		
Surface mail	26	32
Air Mail (outside Europe only)	49	60
Electronic subscription only	21	25
Proceedings of the International Meteor Conference on paper		
1990, 1991, 1993, 1995, 1996, 1999, 2000, 2002, 2003, per year	9	12
2007, 2010, 2011, per year	15	20
2012, 2013, 2014, 2015 per year	25	34
Proceedings of the Meteor Orbit Determination Workshop 2006	15	20
Radio Meteor School Proceedings 2005	15	20
Handbook for Meteor Observers	15	20
Meteor Shower Workbook	12	16
Electronic media		
Meteor Beliefs Project ZIP archive	6	8

2019 September 27 fireball from Germany

Fireball from 2019 September 27, $17^{h}29^{m}$ UT captured from Ketzür, Germany. Top image: fireball start and most of the fireball trail as recorded by camera 2 of AllSky6 camera AMS16. Bottom image: cropped frames from camera 1 of AllSky6 camera AMS16, showing the last part of the fireball with multiple fragments. Both images courtesy of Sirko Molau.

The IMO received 221 reports of this event 2019-4624:
`https://fireball.amsmeteors.org/members/imo_view/event/2019/4626`.